Infectious disease modeling and innate immune function in zebrafish embryos

Cui, C.; Benard, E.L.; Kanwal, Z.; Stockhammer, O.W.; Vaart, M. van der; Zakrzewska, A.; ... ; Meijer, A.H.

CHAPTER 12

Infectious Disease Modeling and Innate Immune Function in Zebrafish Embryos

Chao Cui, Erica L. Benard, Zakia Kanwal, Oliver W. Stockhammer, Michiel van der Vaart, Anna Zakrzewska, Herman P. Spaink and Annemarie H. Meijer

Institute of Biology, Leiden University, Leiden, The Netherlands

Abstract

The major cell types of the innate immune system, macrophages and neutrophils, develop during the first two days of zebrafish embryogenesis. The interaction of these immune cells with pathogenic microbes can excellently be traced in the optically transparent zebrafish embryos. Various tools and methods have recently been developed for visualizing and isolating the zebrafish embryonic innate immune

METHODS IN CELL BIOLOGY, VOL 105

0091-679X/10 $35.00
DOI 10.1016/B978-0-12-381320-6.00012-6

cells, for establishing infections by different micro-injection techniques, and for analyzing the host innate immune response following microbial recognition. Here we provide practical guidelines for the application of these methodologies and review the current state of the art in zebrafish infectious disease research.

I. Introduction

Over the recent years, the zebrafish has firmly gained ground as a model for inflammatory and infectious diseases. A rapidly growing list of human pathogens or closely related animal pathogens has been used for experimental infections in zebrafish (Allen and Neely, 2010; Kanther and Rawls, 2010; Lesley and Ramakrishnan, 2008; Meeker and Trede, 2008; Meijer and Spaink, 2011; Sullivan and Kim, 2008). Tuberculosis and other human infectious diseases can be modeled in zebrafish either using adult individuals with a fully developed adaptive immune system or using embryos and larvae that have developed only innate immune cell types. Microarray and deep sequencing technologies have been instrumental to characterize immune responses to different types of infection. These studies have demonstrated the induction of transcriptional regulators and immune effectors that are highly conserved between zebrafish and human (Meijer and Spaink, 2011). In addition, functional studies have shown that central signaling pathways of the innate immune system are already operational during infections in 1-day-old embryos and subsequent larval stages (Aggad *et al.*, 2010; Clay *et al.*, 2008; Stockhammer *et al.*, 2009).

The zebrafish offers significant advantages for studying host–pathogen interactions. First, due to their optical transparency, zebrafish embryos are highly suited for live imaging of chemotaxis, phagocytosis, and pathogenesis. As further discussed below, these studies are greatly facilitated by transgenic reporter lines expressing fluorescent proteins in different immune cell types and by specific immune response assays that can be performed *in vivo*. Second, the large number of offspring, the short generation time, and the high-quality genome sequence of zebrafish enable the rapid accumulation of loss- or gain-of-function mutants using forward or reverse genetic screening approaches (Amacher, 2008; Haffter and Nusslein-Volhard, 1996; Wienholds *et al.*, 2002). Morpholino technology provides an efficient complementary tool for transient gene knockdown in embryos until larval stages (Nasevicius and Ekker, 2000). Finally, a major strength of the zebrafish model has come from the opportunity to study early developmental stages of the innate immune cells, which are barely accessible in classical vertebrate models (Traver *et al.*, 2003; Trede *et al.*, 2004). Because of these special features, the zebrafish model is a valuable addition to mammalian models for vertebrate immunology, and an excellent screening tool to define novel factors that participate in host–pathogen interactions.

The innate immune system, which can be classified into physical barriers, cellular, and humoral components, controls the first line of defense against infections. Functional phagocytes, complement factors, and antimicrobial enzymes are present in the embryo before or soon after hatching (Herbomel *et al.*, 1999; Traver *et al.*,

2003; Trede *et al.*, 2004). Recognition of microbes by the innate immune system is mediated by the germline-encoded pattern recognition receptors (PRRs), which are located on the cell surface, on endosomal compartments, and in the cytosol. PRRs recognize pathogen-associated molecular patterns (PAMPs) and intracellular chemical components released through injury or infection (Mogensen, 2009). The best studied family of PRRs is that of the Toll-like receptors (TLRs) (Coban *et al.*, 2009). Putative orthologs of the mammalian TLRs and many downstream signaling intermediates as well as other PRRs, such as the NOD receptors, have been identified in zebrafish (Jault *et al.*, 2004; Meijer *et al.*, 2004; Stein *et al.*, 2007). Microbe recognition by PRRs directly initiates specific signal transduction cascades that not only activate innate effector mechanisms but also function to alert the adaptive immune system (T- and B-cell-mediated immunity). However, in zebrafish the adaptive immune system is not fully matured until approximately 4 weeks postfertilization (Lam *et al.*, 2004). This temporal separation between the two branches of the immune system makes zebrafish embryos and larvae highly suitable for analyzing the innate host factors involved in the interaction with pathogens.

Several detailed reviews of zebrafish as an experimental infection model have been published in the last few years (Kanther and Rawls, 2010; Lesley and Ramakrishnan, 2008; Meeker and Trede, 2008; Meijer and Spaink, 2011; Sullivan and Kim, 2008). In this chapter, our main goal is to give practical guidelines for infection studies in zebrafish embryos. In the following sections, we provide a brief summary of innate immune cell development in zebrafish, followed by an overview of tools and methods used for visualizing specific immune cell populations in embryos. We then describe various strategies to achieve systemic or local infection of embryos with bacterial pathogens, and we discuss quantification methods to analyze bacterial burden at low- or high-throughput levels. Finally, we provide advice on the use of transcriptomic technologies for characterizing innate immune responses and discuss functional studies of some key factors in the innate immune system. For additional reading, we recommend other highly useful methods papers on the analysis of innate immunity in zebrafish (Hall *et al.*, 2009; Herbomel and Levraud, 2005; Levraud *et al.*, 2008; Mathias *et al.*, 2009).

II. Observation and Isolation of Innate Immune Cells

A. Innate Immune Cell Development in Zebrafish

The majority of innate immune cell types, including the phagocytic cells, belong to the myeloid cell lineage, but natural killer cells, which are of lymphoid origin, also belong to the innate immune system. As in mammals, the development of immune cells during zebrafish embryogenesis occurs in distinct waves of primitive and definitive hematopoiesis (Bertrand and Traver, 2009; Davidson and Zon, 2004). The primitive wave of hematopoiesis begins in the anterior lateral plate mesoderm or rostral blood island, where hemangioblasts differentiate into myeloid cells, and in the posterior lateral plate mesoderm, which gives rise to erythroid cells. A transient

wave of hematopoiesis occurs in the posterior blood island of 1-day-old embryos that contains the first erythromyeloid progenitor cells (EMPs) (Bertrand *et al.*, 2007). The posterior blood island region subsequently expands into the caudal hematopoietic tissue, which forms a transient site of hematopoiesis from where cells further migrate to seed the thymus and pronephros (Murayama *et al.*, 2006). The pronephros develops into the kidney marrow in adult fish and is considered equivalent to mammalian bone marrow (Traver *et al.*, 2003). A final wave of definitive hematopoiesis in the ventral wall of the embryonic dorsal aorta produces cells that have a long-term hematopoietic stem cell potential and that become the founders of the adult hematopoietic system, similar to situation in the mouse embryo (Bertrand *et al.*, 2010; Boisset *et al.*, 2010; Kissa and Herbomel, 2010).

In the zebrafish embryo, the first innate immune cells to differentiate are the primitive macrophages, which migrate to the yolk sac before the onset of blood circulation and subsequently join the blood circulation or invade cephalic mesenchyme, brain, retina, and epidermis (Herbomel *et al.*, 1999, 2001). The next type of immune cells that differentiate are the neutrophils, which have detectable myeloperoxidase (Mpx) enzyme activity and Sudan Black staining cytoplasmic granules by 2 days postfertilization (dpf) (Le Guyader *et al.*, 2008; Lieschke *et al.*, 2001; Willett *et al.*, 1999). As a molecular marker, the enzyme myeloperoxidase (*mpx*) was shown to be expressed only in neutrophils (Bennett *et al.*, 2001; Lieschke *et al.*, 2001). Prior to the maturation of neutrophils, *mpx* messenger RNA is already apparent in a distinct myeloid population at 28 hours postfertilization (hpf) (Zakrzewska *et al.*, 2010). Mast cells, characterized by carboxypeptidase 5 expression, form another myeloid lineage developing from the first day of embryogenesis. Around 60 hpf, macrophages that have previously invaded the brain and retina undergo a phenotypic transition into microglia (Herbomel *et al.*, 2001). Thus, at least four distinct myeloid cell types are present before the first immature lymphocyte precursors appear in the developing thymus around 4 dpf. Two other myeloid cell types have been characterized in adult zebrafish, the eosinophils and a population of antigen-presenting cells similar to the mammalian dendritic cells (Balla *et al.*, 2010; Lugo-Villarino *et al.*, 2010). Based on the expression of characteristic receptor genes, it is presumed that natural killer cells also exist in zebrafish, but these cells remain to be characterized (Yoder *et al.*, 2009). For visualizing different innate immune cell populations during embryonic and larval development, various methods have been established, which will be further described in the following sections.

B. Detection of Immune Cells Using Cell-Specific Markers

1. Colocalization Studies of Immune Cell Markers by *in situ* Hybridization

One of the most basic methods in zebrafish research is the *in situ* study of gene expression patterns in the whole embryo. In whole-mount *in situ* hybridization, gene-specific markers can be used to trace the spatial–temporal distribution of immune cells during their development or in response to infection or wounding. In early zebrafish

embryos, two gene-specific markers have been widely used to distinguish macrophages and neutrophils. The gene *mpx* is currently the most robust marker for detection of neutrophils, whereas the gene encoding colony-stimulating factor 1 receptor (*csf1ra*, previously called *fms*) has been extensively utilized to identify the macrophages (Herbomel *et al.*, 2001; Lieschke *et al.*, 2001). Although the use of *csf1ra* as a macrophage marker has been well documented in previous research, its disadvantage is that it is also expressed in a pigment cell type, the xanthophores. Therefore, the search for marker genes specific only to macrophages has been crucial to facilitate the analysis of macrophage responses to various types of immune system triggers.

Our recent study of early myeloid genes under control of the Spi1 (Pu.1) transcription factor led to the discovery of four novel markers for early zebrafish macrophages, *mfap4*, *mpeg1*, *cxcr3.2*, and *ptpn6* (Zakrzewska *et al.*, 2010). First, to determine that the spatial–temporal expression pattern of these genes resembles that of other myeloid-specific genes such as *lcp1*, *spi1*, and *mpx*, whole-mount *in situ* hybridization with digoxigenin-labeled antisense RNA probes and alkaline phosphatase detection was used. This method has been described in detail elsewhere (Westerfield, 2000). To verify whether these novel marker genes are specifically expressed in macrophages, rather than neutrophils, double fluorescent *in situ* hybridization (FISH) was utilized to determine the overlap with the known marker genes. In the FISH procedure, standard digoxigenin- and fluorescein-labeled probes are combined with tyramide signal amplification (TSA), which increases the signal-to-noise ratio considerably. Horseradish peroxidase (HRP)–conjugated antibodies are used to catalyze the precipitation of the fluorophore-labeled tyramide amplification reagent at the specific sites of mRNA–probe binding. Two variants of the protocol are available (Fig. 1). The one-step procedure utilizes the HRP-conjugated anti-digoxigenin or anti-fluorescein antibodies for detection of the site-specific gene expression. In the two-step procedure, two consecutive antibodies are applied for the detection of each probe, first a sheep anti-digoxigenin or anti-fluorescein antibody and next an HRP-conjugated anti-sheep antibody (Clay and Ramakrishnan, 2005). The one-step procedure is shorter by 2 days than the two-step procedure. However, the two-step procedure appears to be more sensitive due to the additional amplification of the signal by a secondary antibody. TSA amplification systems can be used with Alexa Fluor dyes (Invitrogen) or with Cy dyes and fluorescein (PerkinElmer). We generally use the TSA-Plus systems (PerkinElmer), which provide higher sensitivity than regular TSA, although this also creates higher background, especially in the yolk region. Furthermore, we prefer the combination of a digoxigenin-labeled probe with a red fluorescent dye for the detection of the gene that has the lower expression level of the two genes tested. In these HRP-based double FISH protocols, it is absolutely crucial to inactivate HRP completely using hydrogen peroxide after detection of the first gene. Failure to do so may result in an artifactual overlap of the expression patterns of the two genes tested.

In our study, we performed double FISH on 28 hpf zebrafish embryos, using our genes of interest labeled with digoxigenin and detected with TSA-Plus/Cy3 combined with either *csf1ra* (macrophage marker) or *mpx* (neutrophil marker) labeled

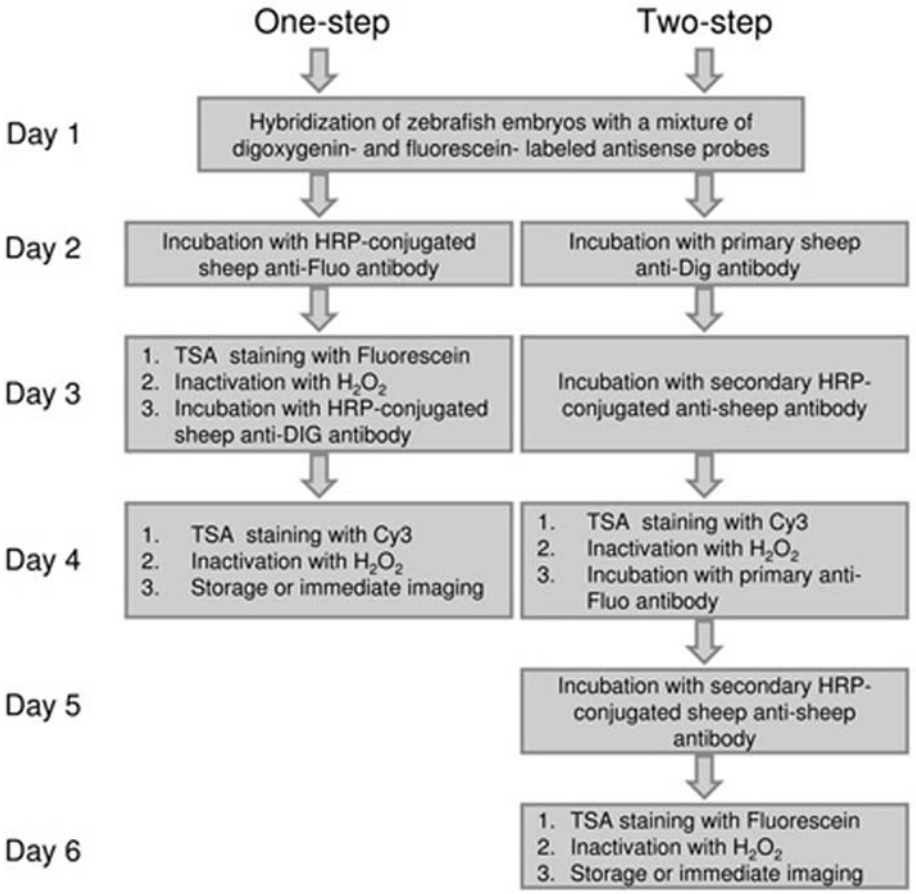

Fig. 1 Schematic representation of the double fluorescent *in situ* hybridization (FISH) protocol. Anti-Dig, anti-digoxigenin; anti-Fluo, anti-fluorescein.

with fluorescein and detected with TSA-Plus/fluorescein. This method allowed us to determine that all four genes identified in this study are expressed specifically in macrophages of 1-day-old embryos and that *mpeg1* and *mfap4* are the most robust and specific markers for detecting macrophages also at later stages of embryonic development. Below we describe the protocols for the one- and two-step double FISH procedures.

Two-Step Double FISH Protocol

Day 1:

1. Fix embryos overnight (O/N) in 4% paraformaldehyde in phosphate buffered saline (PFA–PBS) at 4 °C.

2. Dehydrate embryos using a graded series of PBST/methanol (PBST: 0.1% Tween 20 in PBS) and store in 100% methanol at −20 °C.
3. Rehydrate embryos using a graded series of methanol/PBST solution.
4. Digest embryos in Proteinase K solution (10 μg/mL) in PBST at 37 °C; adjust the time to the embryos' age.
5. Fix embryos in 4% PFA–PBS for 20 min at room temperature (RT) followed by 5 × 5 min washing in PBST at RT.
6. Prehybridize embryos in hybridization mix (HM) buffer (formamide 50%, 5× SSC, Tween 20 – 0.1%, citric acid to pH 6.0) for 2–6 h at 65 °C.
7. Hybridize O/N at 65 °C in HM buffer containing 50 μg/mL heparin (Sigma), 500 μg/mL tRNA (Sigma), and 200 ng of each antisense probe (digoxigenin- and fluorescein-labeled).

Day 2:

8. Remove and store the probe mix in −20 °C for reuse (four to five uses per probe).
9. Wash shortly in prewarmed 100% HM at RT.
10. Wash embryos using a graded series of HM/2× SSCT solutions at 65 °C, 15 min each.
11. Wash embryos 2 × 30 min in 0.2× SSCT at 65 °C.
12. Wash embryos using a graded series of 0.2× SSCT/PBST solution, 10 min each.
13. Block embryos for 2–3 h in blocking buffer (BB, Western Block Reagent, Roche, 1:10 dilution in PBST) at RT.
14. Incubate O/N at 4 °C in a 1/3000 dilution of the sheep anti-digoxigenin antibody (Roche catalog number 11093274910) in BB.

Day 3:

15. Wash 6 × 10 min in PBST at RT.
16. Block embryos for 1 h in BB at RT.
17. Incubate O/N at 4 °C in a 1/200 dilution of HRP-conjugated rabbit anti-sheep antibody (Jackson ImmunoResearch catalog number 313-035-047) in BB.

Day 4:

18. Wash 6 × 10 min in PBST at RT.
19. Incubate embryos in the dark for 20–30 min at RT in a 1/50 dilution of TSA-Plus/Cy3 (PerkinElmer) in the provided amplification buffer.
20. 5× quick rinses in PBST at RT.
21. Incubate for 30 min in 6% H_2O_2 solution at RT.
22. Wash embryos 3 × 10 min in PBST at RT, and check fluorescence.
23. Block embryos for 2–3 h in BB at RT.
24. Incubate embryos O/N at 4 °C in a 1/3000 dilution of sheep anti-fluorescein antibody (Roche catalog number 11426338910) in BB.

Day 5:

25. Wash embryos 6 × 10 min in PBST at RT.
26. Block embryos for 1 h in BB at RT.
27. Incubate O/N at 4 °C in a 1/200 dilution of HRP-conjugated rabbit anti-sheep antibody (Jackson ImmunoResearch catalog number 313-035-047) in BB.

Day 6:

28. Wash embryos 3 × 10 min in PBST at RT.
29. Incubate in the dark for 20–30 min at RT in a 1/50 dilution of TSA-Plus/fluorescein (PerkinElmer) in the provided amplification buffer.
30. Wash embryos 5 × 10 min in PBST at RT.
31. Incubate for 30 min in 6% H_2O_2 solution at RT.
32. Wash embryos 3 × 10 min in PBST at RT and store embryos in fresh PBT at 4 °C or image directly.

One-Step Double FISH Protocol

Refer to the above two-step protocol for the first 11 steps.

12. Incubate O/N at 4 °C in a 1/500 dilution of HRP-conjugated anti-fluorescein POD antibody (Roche catalog number 11426346910).

Day 3:

13. Wash 6 × 10 min in PBST at RT.
14. Incubate embryos in the dark for 30–50 min at RT in a 1/50 dilution of TSA-Plus/fluorescein in the provided amplification buffer.
15. Wash and incubate embryos for 30 min in 6% H_2O_2 solution at RT.
16. Wash embryos 6 × 10 min in PBST at RT.
17. Block embryos for 2 h in BB at RT.
18. Incubate O/N at 4 °C in a 1/500 dilution of HRP-conjugated anti-digoxigenin POD antibody (Roche catalog number 11207733910).

Day 4:

19. Wash embryos 6 × 10 min in PBST at RT.
20. Incubate embryos in the dark for 45–60 min at RT in a 1/50 dilution of TSA-Plus/Cy3 in the provided amplification buffer.
21. Wash embryos 5 × 10 min in PBST at RT.
22. Incubate for 30 min in 6% H_2O_2 solution at RT.
23. Wash embryos 3 × 10 min in PBST at RT and store embryos in fresh PBT at 4 °C or image directly.

2. Identification of Cell Types Using Immunodetection and Histochemical Staining

Antibodies against L-plastin, encoded by the *lcp1* gene, are a useful tool for the rapid detection of all myeloid cell types in the embryo (Mathias *et al.*, 2007). There are also antibodies available for the neutrophil-specific Mpx protein (Mathias *et al.*, 2007), but macrophage-specific antibodies are not yet described. Nevertheless, the combination of L-plastin and Mpx antibodies can be used to distinguish macrophages (L-plastin-positive, Mpx-negative) and neutrophils (L-plastin- and Mpx-positive). Because both of the available antibodies are rabbit polyclonals, this requires that one of the two antibodies is coupled directly to a fluorescent dye, while the second can be detected using a dye-coupled secondary antibody (Mathias *et al.*, 2009). A convenient alternative is to combine L-plastin immunofluorescence staining with a histochemical assay for detection of Mpx activity or with Sudan Black staining for specific detection of neutrophil granules (Le Guyader *et al.*, 2008; Lieschke *et al.*, 2001; Mathias *et al.*, 2009; Fig. 3). A fluorescent detection of Mpx activity can be performed with fluorescein isothiocyanate (FITC)- or Cy3-conjugated tyramide (Le Guyader *et al.*, 2008). Staining for Mpx activity can also be performed using a chromogenic substrate that produces a brown to black precipitate (Lieschke *et al.*, 2001). Due to this dark precipitate in the neutrophils, the immunostaining of the pan-leukocytic L-plastin marker only highlights the macrophage population. Below we provide a protocol for this procedure.

Combined L-Plastin Immunofluorescence and Chromogenic Mpx Activity Detection

Day 1:

1. Fix embryos O/N at 4° C in 4% PFA–PBS.
2. Wash embryos in 1× Trizmal (supplied by Peroxidase (Mpx) Leukocyte Kit, Sigma catalog number 390A) containing 0.01% Tween 20 (TT buffer) for 5 min.
3. Incubate embryos in TT buffer containing 1.5 mg/mL substrate (supplied) and 0.015% H_2O_2 for 5–10 min at 37 °C.
4. Wash embryos 3 × 10 min in PBST (0.1% Tween 20 in PBS), and check Mpx staining.
5. Dehydrate embryos in a graded series of PBST/methanol solution and in 100% methanol O/N at −20 °C.

Day 2:

6. Rehydrate embryos in a graded series of methanol in PBS containing 0.8% Triton X-100 (PBS-TX).
7. Wash 4 × 5 min in PBS-TX.
8. Digest embryos in 10 μg/mL Proteinase K for 10 min at 37 °C followed by quick rinse in PBS-TX.
9. Block embryos with PBS-TX containing 1% BSA for 2 h at RT.
10. Incubate O/N at 4 °C in rabbit anti-L-plastin (Mathias *et al.*, 2007) in BB (1:500 dilution).

Day 3:

11. Quick rinse 3× in PBS-TX followed by 4 × 10 min washes in PBS-TX.
12. Block embryos with PBS-TX containing 1% BSA for 1 h at RT.
13. Incubate for 2 h at RT in Alexa Fluor 488 or 568 goat anti-rabbit (Invitrogen, 1:200).
14. Quick rinse 3× in PBS-TX followed by 3 × 10 min washes in PBS-TX, and store embryos at 4 °C or image directly.

C. Transgenic Reporter Lines for Live Imaging of Immune Cell Behavior

The excellent availability of *in vivo* imaging is one of the biggest advantages of the zebrafish as a vertebrate model to study innate immunity. Transgenic reporter lines expressing fluorescent proteins under the control of leukocyte-specific promoters are ideal tools to study host–pathogen interactions in the zebrafish model. Several valuable transgenic reporter lines are available to visualize immune cells throughout their development (Table I). Myeloid precursor cells can be visualized as early as 1 dpf using GFP expression under control of the *spi1* promoter (Hsu *et al.*, 2004; Ward *et al.*, 2003; Zakrzewska *et al.*, 2010). Early myeloid cells are also labeled in *fli1:EGFP* transgenic fish, in addition to the GFP expression in the vascular system of this line (Redd *et al.*, 2006). Starting at 2 dpf, the *mpx* promoter can be used as a specific marker for neutrophils. Two transgenic lines, produced with different strategies, that use the *mpx* promoter to label the neutrophil population with GFP brightly are available. One of these lines was constructed in the Huttenlocher lab by fusing an 8-kb promoter region to GFP (Mathias *et al.*, 2006). An additional population of low

Table I
Promoter transgenes used for labeling myeloid cells

Promoter	Specificity	Remarks	References
spi1	Early myeloid cells	Visible at 1–2 dpf	Ward *et al.* (2003), Hsu *et al.* (2004)
fli1	Early myeloid cells	Marker for vasculature	Redd *et al.* (2006)
mpx	Neutrophils	Weak fluorescence in macrophages also reported	Mathias *et al.* (2006, 2009), Renshaw *et al.* (2006)
lyz	Neutrophils		Hall *et al.* (2007)
csf1ra	Macrophages	Also labeling xanthophores	Gray *et al.* (2011)
mpeg1	Macrophages		Ellett *et al.* (2010)
cxcr3.2	Macrophages and minor neutrophil subset	Currently under construction	Meijer lab
mych	Subset of neutrophils	YFP enhancer trap line	Meijer *et al.* (2008)
myd88	Subsets of myeloid cells		Hall *et al.* (2009)
apoeb	Microglia		Peri and Nusslein-Volhard (2008)

GFP-expressing cells can be observed in this transgenic line. This population was later characterized as inflammatory macrophages based on morphology, marker gene expression, and behavior (Mathias *et al.*, 2009). The other *mpx:GFP* neutrophil line was created in the Renshaw lab using a BAC recombineering strategy, which replaced the coding sequence of the gene with GFP and therefore maintained the entire promoter region (Renshaw *et al.*, 2006). The Renshaw lab has not reported an additional population of low GFP-expressing inflammatory macrophages in this line. In our laboratory, this line also appears exclusively neutrophil-specific, but others observed a low GFP-expressing macrophage population, suggesting that some differences in expression may have arisen in different offspring from the original line (Ellett *et al.*, 2010). Using promoter fragments of the lysozyme C (*lyz*) gene, *lyz:EGFP/DsRED2* transgenes have been created that display a significant overlap with the *mpx:GFP* transgene expression (Hall *et al.*, 2007). Although originally reported to label a macrophage subset too, *lyz* is thought to drive neutrophil-specific expression, based on several reports (Ellett *et al.*, 2010; Meijer *et al.*, 2008). A transgenic line that specifically labels macrophages has long been awaited. Recently, a BAC recombineering strategy has been used to create a transgenic line for the macrophage-specific marker *csf1ra* (*fms*) (Gray *et al.*, 2011). Despite the fact that it also shows transgene expression in xanthophores, this line has great potential for use, together with the *mpx:GFP* lines, in live imaging studies of macrophage and neutrophil behavior. The zebrafish genes *mfap4*, *mpeg1*, *cxcr3.2*, and *ptpn6* have recently been identified as early macrophage-specific marker genes, not showing the additional xanthophore expression (Zakrzewska *et al.*, 2010). In an independent study, the Lieschke lab used the promoter sequence of the *mpeg1* gene to create the first entirely macrophage-specific transgenic lines (Ellett *et al.*, 2010). In collaboration with the Renshaw lab, we have a *cxcr3.2* reporter line under construction. The preliminary analysis of a BAC recombineering transgene construct shows that it is expressed in macrophages and a small subset of *mpx:GFP*-expressing neutrophils, making it an interesting marker to further investigate various myeloid subsets. Other lines that label subsets of myeloid cells include the *Et(CLG-YFP)smb463* line (CLGY463), which has a YFP enhancer trap insertion close to a member of the *myc* gene family (*mych*) (Meijer *et al.*, 2008), and the *myd88:EGFP* and *myd88:DsRED2* lines, which have fluorescent protein expression driven by the promoter of *myd88*, a key adaptor molecule in TLR signaling (Hall *et al.*, 2009). Introduction of a membrane-bound GFP into the apolipoprotein E (*apoeb*) locus resulted in a transgenic line that labels zebrafish microglia (Peri and Nusslein-Volhard, 2008). Generating transgenic lines not only is useful to visualize subsets of innate immune cells but can also be used to create reporter lines for transcription factors or chemokines that are important in innate immunity, such as NFκB or IL-8 (also known as CXCL8) (Kanther and Rawls, 2010). The creation of such reporter lines will be of great help in studies of the dynamics of the innate immune response.

The Gal4/upstream activating sequence (UAS) two-component system provides a highly versatile toolbox for transgene expression (Halpern *et al.*, 2008). The first component of this system, the so-called transgenic driver line, consists of a cell- or

tissue-specific promoter that drives the expression of the yeast Gal4 transcription factor. The second component is a fish line that contains a transgene under the control of the UAS of Gal4. When these two transgenic fish lines are crossed, the transgene under the control of UAS will be expressed only in those cells where the cell- or tissue-specific promoter that drives Gal4 is active. With this system, it is possible to drive transgene expression in different leukocyte subsets. A large variety of UAS lines is available, which can be used for different purposes. For example, a *UAS:Kaede* line highlights cells by green fluorescence. The green fluorescent Kaede protein can be photoconverted into its red fluorescent form by exposing it to UV light (Halpern *et al.*, 2008). This photoconversion can be used, for example, to visualize the dynamics of arriving and departing leukocytes at a site of infection, by photoconverting the Kaede proteins in cells in that area into their red fluorescent form (Ellett *et al.*, 2010). A second example of the usefulness of this system is the possibility to ablate subsets of cells or entire tissues specifically. This can be done by combining a Gal4 line specific for the target cells with the *UAS:NfsB-mCherry* line, which drives expression of the *E. coli* gene *nitroreductase B* (Halpern *et al.*, 2008). Nitroreductase B is an enzyme that can convert precursor drugs such as metronidazole into toxic cellular metabolites. The cells that are targeted for ablation by nitroreductase B are simultaneously made visible, due to the fusion of nitroreductase B with mCherry protein. This strategy was used to ablate macrophages specifically, without significantly altering neutrophil numbers (Gray *et al.*, 2011). An alternative strategy for cell ablation is light-induced killing using the *UAS:KillerRed* line (Del Bene *et al.*, 2010). Creating Gal4 driver and UAS reporter lines has become more efficient by the introduction of Tol2-based vectors, the use of which leads to high rates of genomic integration when co-injected with Tol transposase mRNA (Suster *et al.*, 2009). A potential problem when using the Gal4/UAS system is that silencing of the UAS sequence might occur over subsequent generations, making it necessary to regenerate UAS lines frequently.

D. Isolation of Immune Cells from Reporter Lines

The zebrafish transgenic lines with fluorescently labeled immune cells can be utilized conveniently for the isolation of specific populations of immune cells based on their fluorescent characteristics. In our recent study of Spi1-dependent genes expressed in early zebrafish myeloid cells, we performed transcriptome profiling of myeloid cells that were obtained from *spi1:GFP* embryos by fluorescence-activated cell sorting (FACS). For preparation of a single-cell suspension for FACS sorting, the embryos were digested with trypsin. The removal of yolk prior to trypsin treatment drastically reduces the amount of debris in the single-cell suspension, therefore providing better resolution and faster sampling during FACS. The number of embryos required for FACS sorting and subsequent applications depends on the expected percentage of fluorescent cells per embryo. In the case of the *spi1:GFP* line used in our study, which shows some additional brain-specific GFP expression, there are on average 1.5% GFP+ (expressing) cells per 28–30 hpf embryo. Approximately

300 embryos gave a standard yield of approximately 2×10^5 GFP+ cells, from which sufficient RNA could be obtained for microarray hybridization using the Ambion RNAqueous Microkit and a single round of RNA amplification. As discussed in the section "Transcriptomic Analysis," it is also possible to use less starting material and an extra round of RNA amplification. Our protocol for obtaining single-cell suspensions and FACS sorting follows here (based on Covassin *et al.*, 2006).

1. Embryo Dissociation for FACS

1. Collect 300–600 embryos at the desired developmental stage (depends on the expected percentage of fluorescent cells per embryo, 300–600 embryos work fine for 1.5% GFP-positive cells).
2. Dechorionate embryos by treatment with freshly prepared 2 mg/mL pronase (Sigma catalog number P5147) in egg water (60 μg/mL sea salts), for 1 min at 28.5 °C.
3. Rinse the embryos in calcium-free Ringer solution for 15 min and pass them several times through a 200-μL pipette tip to remove the yolk.
4. Transfer the embryos into a 35-mm culture dish with 2 mL PBS (PBS, pH 8) containing 0.25% trypsin and 1 mM EDTA.
5. Incubate 90 min at 28.5 °C (depends on the number of embryos, this time works for 300 embryos of 28 hpf); during incubation pass samples through a 200-μL pipette tip every 10 min in order to triturate embryos into a single-cell suspension.
6. Stop the digestion by adding $CaCl_2$ to a final concentration of 1 mM and fetal calf serum to 10%.
7. Centrifuge the cells for 3 min at $1000 \times g$.
8. Rinse the cells with PBS once and repeat centrifugation.
9. Resuspend the cells at $\sim 10^7$ cells/mL in Leibovitz medium L15 without phenol red, 10% fetal calf serum, 0.8 mM $CaCl_2$, penicillin 50 U/mL, and streptomycin 0.05 mg/mL.
10. Immediately proceed with FACS.

2. FACS

1. During FACS, cells are separately collected in L15, 0.8 mM $CaCl_2$, 10% fetal calf serum, 10% zebrafish embryo extract, penicillin 50 U/mL, and streptomycin 0.05 mg/mL.
2. Immediately proceed with RNA extraction.

3. RNA Extraction from FACS-Sorted Cells

1. Pellet the cells by centrifugation at $12{,}000 \times g$ for 4 min.
2. Remove supernatant.
3. Use RNAqueous Microkit (RNAqueous®-Micro Kit, Ambion catalog number AM1931) according to the protocol.

III. Bacterial Infection Methods

A. Routes of Infection

The infection of zebrafish embryos is usually initiated by injecting the infectious agent into the host via different sites, depending on the type of experiment to be performed. Borosilicate glass capillary needles (1 mm O.D. × 0.78 mm I.D.), equivalent to those used for injecting morpholinos, are prepared using a micropipette puller and loaded with the inoculum using a microloader tip. The loaded needle is mounted onto a micromanipulator and positioned under the stereomicroscope. The injection time and pressure are set to obtain the correct injection volume, because these values will differ for each needle used. The diameter for a drop of 1 nL is 0.62 nm ($V = 4/3\pi r^3$). The drop size is adjusted to match the desired diameter with the help of a scale bar on a microscope slide or in the ocular. The micromanipulator with the loaded needle is set into the correct position prior to injections and is only moved up and down to inject. The injection plate containing embryos is moved by hand during injections to orientate the embryos into the preferred position for injection. Except when the yolk is used as the injection site, the embryos are dechorionated prior to injection and kept in a Petri dish filled with egg water (60 μg/mL sea salts) and with a layer of 1% agarose on the bottom to prevent embryos from sticking to the plastic surface. Embryos can be anesthetized with 200 μg/mL buffered 3-aminobenzoic acid (tricaine, Sigma–Aldrich). If required for subsequent imaging, 0.003% 1-phenyl-2-thiourea (PTU, Sigma) can be added to prevent melanization. Below we give guidelines for different injection procedures that we have used to achieve systemic or local infection with bacterial pathogens, but these methods can also be applied for injection of viruses, fungal spores, or protozoan parasites. The best positioning of the injection needle during these procedures is illustrated in Fig. 2. For bacterial injections, we check the amount of colony-forming units (cfu) injected into the embryos, by injecting the same inoculum directly into a sterile PBS drop on growth medium. This drop is then plated out and the bacterial colonies are counted after incubation. Because the immune system becomes increasingly competent during embryo development, the proper staging of embryos is very important to compare results among different infection experiments (Kimmel *et al.*, 1995).

1. Yolk Injection

The yolk is a convenient injection site that can be used to achieve systemic infection with slow-growing bacteria such as *Mycobacterium marinum*, which have a generation time of approximately 6-8 h. However, with other pathogens, for instance, *Salmonella typhimurium*, yolk injection leads to rapid proliferation and early lethality of the embryo. We have found that yolk injection of *M. marinum* during the first hours of embryogenesis, from the 16-cell stage onwards, does not interfere with embryo development. To prevent their immediate diffusion, the bacteria are resuspended in 2% polyvinylpyrrolidone (PVP_{40}) prior to yolk injection. During

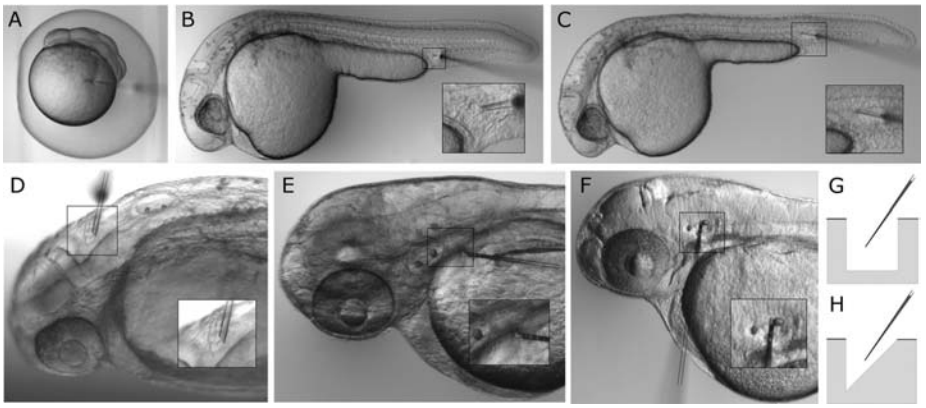

Fig. 2 Injection sites to initiate systemic (A, B, and E) or local (C, D, and F) bacterial infection in the zebrafish embryo. (A) Yolk injection at 16-cell stage. (B) Posterior blood island and (C) tail muscle injection at 28 hpf. (D) Hindbrain ventricle injection at 28 hpf. (E) Duct of Cuvier injection at 54 hpf. (F) Otic vesicle injection at 54 hpf. (G) An agarose plate with rectangular channels can be used for yolk, tail muscle, and otic vesicle injections. (H) An agarose plate with triangular channels can be used for hindbrain injection by positioning the embryo with its ventral side against the vertical wall of the channel and the dorsal side against the slanted wall facing up toward the needle. For the posterior blood island and duct of Cuvier injections, embryos can simply be placed on flat agarose plates.

the first days of embryogenesis, the *M. marinum* bacteria disseminate from the yolk into the tissues, resulting in a similar infection phenotype as on the intravenous route of infection described below (Carvalho *et al*., 2011). In collaboration with the company ZFscreens, our laboratory has developed an automated injection system for yolk injections, which supports high-throughput assays (Carvalho *et al*., 2011).

2. Tail Muscle Injection

To examine immune cell migration toward a local bacterial infection, injection can be conducted in the tail muscle of 1-day-old embryos where macrophages are normally not present. Muscle injections can also be performed at later stages when neutrophils have differentiated. Because the injection location is chosen just above the blood island (or later caudal hematopoietic region) located behind the urogenital opening, it can rapidly induce the migration of innate immune cells. This injection location is also convenient to compare the number of migrated cells relative to the total number of innate immune cells in the tail (Zakrzewska *et al.*, 2010). To perform the injection, the anesthetized embryos are oriented horizontally on a flat 1% agarose plate with the tail pointing toward the needle as shown in Fig. 2C. A volume of 5 nL of bacterial inoculum in PBS can be injected into the muscle above the urogenital opening without causing damage to the notochord and blood vessels. In muscle injections of 28 hpf embryos, we have observed that two distinct myeloid cell populations are attracted to the infection site, one expressing *mpx* and the other

expressing macrophage markers (Zakrzewska *et al.*, 2010). Knockdown of the chemokine receptor *cxcr3.2* specifically reduced migration of the population expressing the macrophage markers (Zakrzewska *et al.*, 2010). Although the injection of PBS buffer alone also attracts some myeloid cells due to muscle tissue damage, the effect of *cxcr3.2* knockdown was specifically related to the migration of macrophages to bacteria.

3. Hindbrain Ventricle Injection

The hindbrain ventricle is a closed cavity of the embryo that contains zero to two macrophages at 30 hpf (Davis *et al.*, 2002; Herbomel *et al.*, 1999). The migration of macrophages following injection of bacteria into this cavity has been documented in several studies (Clay *et al.*, 2007; Davis *et al.*, 2002; Herbomel *et al.*, 1999). For example, injection of 20–100 *M. marinum* bacteria rapidly induced macrophage recruitment into this area (Davis *et al.*, 2002). Because the size of the hindbrain cavity is limited, not more than 0.5–1 nL should be injected. For hindbrain injections, we recommend to line up the anesthetized embryos on a 1% agarose injecting plate with *V*-shaped channels. A description of the plastic mold to make these channels can be found in *The Zebrafish Book* (Westerfield, 2000), also available on the ZFIN website (zfin.org). The embryos are positioned and orientated with their ventral side toward the vertical wall of the channel (Fig. 2D). The needle is inserted into the hindbrain ventricle from an anterior position without touching the underlying neuroepithelium and the bacteria are injected. For practicing the procedure, it is convenient to use a fluorescent dye, which will reveal possible damage of the underlying tissue (Gutzman and Sive, 2009; Levraud *et al.*, 2008).

4. Otic Vesicle Injection

For embryos older than 48 hpf, another suitable body cavity for bacterial injection is the otic vesicle due to its increasing size during development. For otic vesicle injections, anesthetized embryos are positioned laterally on a flat 1% agarose plate with just enough egg water to create surface tension to hold the embryos in place on the agarose layer during injections (Fig. 2F). Puncture of the vesicle has to be conducted with extra care to avoid local tissue rupture, which by itself will result in a massive attraction of immune cells. If carefully performed, PBS injection into the otic vesicle induces no or only minor cell migration, whereas the injection of various bacteria such as *E. coli*, *M. marinum*, and *S. typhimurium* specifically attracts both macrophages and neutrophils (Carvalho *et al.*, 2011; Le Guyader *et al.*, 2008). To avoid wounding effects, the injection volume should be limited to 1 nL (Levraud *et al.*, 2008). We generally use approximately 20 bacteria for injection. We prefer to inject between 2 and 3 dpf, because the epithelium of the otic vesicle becomes more difficult to penetrate at later stages.

5. Systemic Infection via the Blood Island

A systematic infection of 1-day-old embryos can be obtained by injecting bacteria into the blood circulation at the blood island. We usually perform these infections at 28 hpf, shortly after the onset of circulation. The anesthetized embryos are lined up on a flat 1% agarose injecting plate with their tails pointing toward the tip of the needle (Fig. 2B). As mentioned above, only a limited amount of egg water is used to keep the embryos in place on flat agarose plates. The periderm is pierced with the needle tip, and bacteria are injected directly into the caudal vein close to the urogenital opening. The injected volume will always follow the blood flow throughout the caudal vein toward the heart and can be monitored directly after the pulse by the expanding volume within the vascular system (Davis *et al.*, 2002).

6. Infection via Duct of Cuvier

Alternatively to blood island injection, bacteria can also be introduced into the blood circulation via injection at the duct of Cuvier, which is the wide blood circulation valley on the yolk sac connecting the heart to the trunk vasculature. The duct of Cuvier can be used for injections between 1 and 3 dpf. As for blood island injections, the anesthetized embryos are lined up on a flat agarose plate, their tails pointing toward the needle. The needle is inserted into the starting point of the duct of Cuvier just dorsal to the location where the duct starts broadening over the yolk sac (Fig. 2E). This location is the deepest section of the duct and therefore provides the lowest risk of puncturing the yolk sac. The bacterial inoculum will follow the blood flow through the duct of Cuvier over the yolk sac toward the heart and can be monitored directly after the injection by the expanding volume within the duct.

B. Quantification of Bacterial Burden

1. CFU Determination

The most straightforward approach to determine the bacterial burden of infected zebrafish embryos is to quantify the amount of cfu by plating on a suitable growth medium. Commonly, a group of five embryos is triturated by repetitively pipetting the embryos up and down in a volume of 100 μL PBS containing 1% Triton X-100 (van der Sar *et al.*, 2003). Alternatively, embryos can be placed in a 2-mL Eppendorf tube and disrupted by addition of a metal bead (4 mm diameter, Fabory) followed by shaking for 1 min at maximum frequency in a grinder such as the MM 301 mixer mill (Retsch). Subsequently, serial dilutions are cultured on appropriate selection agar plates for cfu assessment. However, a common problem with slow-growing bacteria such as *M. marinum* is the growth competition by the natural microbial flora of the zebrafish embryo. A strategy to overcome this problem in the case of mycobacterial infections is the use of the BBL® MycoPrep™ Kit (BD Biosciences catalog number 240862). After dissociation of embryos in PBS containing 0.1% Triton X-100, the samples are incubated for 9 min in 100 μL MycoPrep reagent and subsequently

plated on selection plates (Clay *et al.*, 2007). Besides being labor intensive, this and other methods for cfu determination will not allow following the progression of bacterial infection of a distinct embryo over time.

2. Pixel Count Analysis Using Fluorescent Images

A convenient alternative to cfu counts is pixel count analysis. Taking advantage of fluorescently labeled bacteria, it is possible to follow the progression of the infection over time. Counting the amount of fluorescent pixels for each embryo, the bacterial burden can be expressed in relative units and different treatment groups can be compared. For example, in *M. marinum* infection experiments, the results of pixel quantification have been shown to correlate well with cfu determination (Tobin *et al.*, 2010). Pixel quantification can be performed with various image analysis software programs, for example, the freeware program ImageJ. A program specially developed for the analysis of zebrafish embryos proved very useful for the batchwise analysis of images of infected embryos in an *M. marinum* mutant screen (Stoop *et al.*, 2011).

3. High-Throughput Quantification Using the COPAS System

High-throughput detection of the bacterial load of single embryos can be carried out by the complex object parametric analyzer and sorter (COPAS). The COPAS™ XL (Union Biometrica) large particle sorter has been designed for the analysis, sorting, and dispensing of objects up to 1.5 mm in diameter based on size, optical density (OD), and fluorescence intensity. It is equipped with 488- and 561-nm solid state lasers. Up to 8000 data points per embryo can be simultaneously detected and analyzed to set sorting parameters based on the fluorescence profiles in two channels. Prior to analysis, embryos older than 24 hpf and younger than 48 hpf need to be removed from the chorion and kept sedated using 0.02% tricaine to prevent attachment of the embryos to the tubing. The parameters for the analysis need to be set depending on the fluorescent label of the bacterial strain used. In a standard analysis using *M. marinum* (Carvalho *et al.*, 2011), time of flight (TOF), indicating the axial length of an embryo, is set against optical extinction (EXT), indicating the size and internal structure of the embryo. This will allow discrimination between live and dead embryos. Simultaneously, the peak width of the green (510/23 band-pass filter) or red (615/24 band-pass filter) channel is set against the peak height of the same channel to determine the population of infected embryos according to the distribution of the fluorescent signal over the embryo. An infection caused by *M. marinum* will lead to spatially restricted sites of bacterial accumulation and infected embryos will therefore show high but narrow peaks. To define the sorting parameters for the first time, it is necessary to run the samples through the system once to create a profile before starting the analysis. After the profile is set, the samples can be analyzed and sorted into 96-microwell plates. A profile of each embryo showing the distribution of the fluorescent signal across the embryo will be created and the

measured values of the fluorescent signal (given in millivolts) are stored in a spreadsheet for subsequent analysis. The COPAS procedure needs to be optimized according to the specific properties of the pathogen, the type of assay that is used, and the information that needs to be gathered. In addition, due to proliferation of the bacteria and size increase of the embryos, a profile needs to be defined for each analysis time point separately.

C. Model Systems for Infectious Diseases

As summarized in recent reviews, the number of zebrafish infection models for bacterial pathogens has rapidly expanded during the recent years (Allen and Neely, 2010; Kanther and Rawls, 2010; Lesley and Ramakrishnan, 2008; Meeker and Trede, 2008; Meijer and Spaink, 2011; Sullivan and Kim, 2008). Bacterial virulence factors and host immune response genes have been the focus of many investigations in these models. Real-time analyses of the interaction between intracellular bacterial pathogens and host phagocytes have demonstrated that hallmarks of different host–pathogen interactions are reproduced in zebrafish embryos (Davis *et al.*, 2002, 2009; Davis and Ramakrishnan, 2009; Levraud *et al.*, 2009; van der Sar *et al.*, 2003; Vergunst *et al.*, 2010). Below we provide guidelines on how to perform infections with *S. typhimurium* and *M. marinum*, as two representative examples of bacterial pathogens that produce acute and chronic infections in zebrafish embryos, respectively.

1. *S. typhimurium* Infections

S. enterica serovar Typhimurium (*S. typhimurium*) is a good model for the study of Gram-negative infections in zebrafish. Two strains of *S. typhimurium* have been studied in detail, the wild-type SL1027 strain and its isogenic derivative SF1592 (Ra), which is defective in the synthesis of the O-antigen side chain of the outer membrane lipopolysaccharide (LPS). Using wild-type and Ra mutant bacteria containing the DsRed expression vector pGMDs3, it was shown that the wild-type strain induces a rapid lethal infection, whereas infection with the Ra strain is transient and nonpathogenic in zebrafish embryos (van der Sar *et al.*, 2003). A time-course transcriptome profiling study of infection of 28 hpf embryos with the wild-type strain showed a gradual increase of the expression levels of innate immune response genes up to 24 h, at which time point this infection becomes lethal. The gene expression profile was consistent with a strong inflammatory response in these embryos, showing high induction levels of genes such as interleukin 1 beta (*il1b*) and matrix metalloproteinase 9 (*mmp9*), as well as other genes. The Ra strain induced a similar but attenuated response during the first 8 h of the infection, with significantly lower induction levels of these inflammatory genes, and a clear decline of the response was observed at 24 h (Stockhammer *et al.*, 2009). This nonpathogenic strain proved useful for demonstrating the immunocompromised phenotype of zebrafish embryos impaired in innate immunity signaling (van der Sar *et al.*, 2006).

In the laboratory, *S. typhimurium* stocks are kept at −80 °C. For injections, bacteria are freshly grown O/N at 37 °C on LB agar plates supplemented with 100 μg/mL carbenicillin to select for the DsRED expression vector. Individual colonies are picked and resuspended in sterile PBS. To avoid clumping of the bacteria, the suspension should be vortexed well before loading into the microcapillary pipettes. Embryos grown at 28.5–31 °C in egg water are dechorionated, staged at 28 hpf according to their morphological criteria (Kimmel *et al.*, 1995), and injected with approximately 250 cfu into the blood island as described above. Due to the relatively large size of *S. typhimurium* bacteria and their bright DsRED fluorescence, individual bacteria can easily be counted with a fluorescence stereomicroscope to set the injection dose. For verification, an injection drop is also spotted onto LB agar plates and incubated at 37 °C O/N for cfu counting. Individual DsRED *S. typhimurium* cells can be observed circulating in the bloodstream directly after injection, and embryos not properly injected are discarded. Injected embryos are transferred into fresh egg water in agarose-coated plates and are incubated at 28 °C. For survival curves or real-time imaging, embryos are monitored every few hours (wild type) and daily (Ra) after infection.

2. *M. marinum* Infections

M. marinum is an excellent model for human tuberculosis research. *M. marinum* and *M. tuberculosis* are genetically closely related species that cause similar pathological hallmarks in their natural hosts, fish and human (Tobin *et al.*, 2010). They both survive within macrophages and induce the formation of granulomas, which are complex structures of immune cells that provide a niche for the long-term persistence of these pathogens inside their respective hosts (Russell, 2007; Tobin and Ramakrishnan, 2008). The structure of *M. marinum*–induced granulomas in adult zebrafish highly resembles that of human tuberculous granulomas (Swaim *et al.*, 2006). Importantly, it has been shown that the context of the innate immune system of zebrafish embryos is sufficient to initiate granuloma formation (Davis *et al.*, 2002). Following infection by *M. marinum* bacteria at 1 dpf, tight aggregates of infected and noninfected macrophages are observed within several days. Furthermore, granuloma-activated genes (*gag* genes) of *M. marinum*, which are genes that are activated only when the bacteria are contained inside a granuloma, are also activated in these embryonic macrophage aggregates (Davis *et al.*, 2002). The process of macrophage aggregation into initial granulomas has been documented in a detailed manner by real-time imaging (Davis and Ramakrishnan, 2009). Wild-type (M-strain) and mutant strains labeled with many useful fluorescent constructs have been produced by the Ramakrishnan laboratory, which has pioneered the use of this model. For example, *M. marinum* bacteria labeled with the photoconvertible Kaede protein were used to trace how secondary granulomas are seeded from a primary granuloma by egression of single infected macrophages (Davis and Ramakrishnan, 2009). A mutant defective in the ESX-1/RD-1 secretion system, which is conserved between *M. marinum* and *M. tuberculosis*, shows a significantly reduced formation of granulomas and is

attenuated compared to wild-type bacteria, indicating that granuloma formation is part of the virulence mechanism (Volkman *et al.*, 2004, 2010). Another attenuated mutant, *erp*, has a cell wall defect that reduces its growth inside macrophages (Cosma *et al.*, 2006). In functional studies of host genes, this mutant is useful to score effects on bacterial burden of individual infected macrophages by fluorescence microscopy, which is not possible using wild-type bacteria due to their rapid growth kinetics (Clay *et al.*, 2008). Other *M. marinum* strains originating from infected humans or fish have been described that showed marked differences in pathogenicity and induced host gene responses, such as the Mma20 and E11 strains (van der Sar *et al.*, 2004, 2009). *M. marinum* strains can be grown either on Middlebrook 7H10 agar (Difco) plates or in Middlebrook 7H9 liquid medium. For infecting zebrafish embryos, we generally use bacteria grown O/N in 7H9 liquid medium supplemented with ADC, 0.05% Tween 80, and antibiotics (50 μg/mL hygromycin or 20 μg/mL kanamycin) dependent on the fluorescent plasmid used. It is not possible to set the injection dose of *M. marinum* bacteria by counting under the fluorescence stereomicroscope like we do for *S. typhimurium*, as described above. Therefore, the injection dose is based on a standard curve of growth. The generation time of *M. marinum* is approximately 12 h, varying according to the strain. The OD of the bacteria is measured at 600 nm. An OD of 1 at 600 nm corresponds to approximately 1×10^8 *M. marinum*/mL (this may vary according to the bacterial strain used). When the bacteria are in logarithmic phase (OD_{600} should not exceed 1.00), they are harvested by centrifugation and washed three times with PBS. The OD_{600} is measured again and the suspension is diluted to the desired concentration of cfu. For injections, we prefer to centrifuge this suspension and resuspend the pellet in 2% PVP_{40}, which we find improves homogeneity of the suspension resulting in more reproducible inocula. The standard route for infecting embryos is blood island injection, as described above. We generally inject a dose of 150–200 cfu in 1 nL. For high-throughput applications such as drug screening, injection of approximately 40 cfu into the yolk around the 16-cell stage or later proved useful (Carvalho *et al.*, 2011). This method results in the formation of granulomas in the head, body, and tail of the larvae, similar as with the conventional blood island infection route.

IV. Analysis of the Innate Immune Response

A. Bioassays for the Innate Immune Response

The production of reactive oxygen and nitrogen species is a major effector mechanism of the innate immune response. The respiratory burst in zebrafish embryos can be determined by an assay that measures the oxidation of the nonfluorescent dye 2′,7′-dihydrodichlorofluorescein diacetate (H2DCFDA) to the fluorescent product dichlorofluorescein (DCF) (Hermann *et al.*, 2004). In addition, nitric oxide production can be visualized in living zebrafish embryos using diaminofluorophore 4-amino-5-methylamino-2′-7′-difluorofluorescein diacetate (DAF-FM-DA) as a cell-permeant probe (Lepiller *et al.*, 2007).

B. Transcriptomic Analysis

Microarray and deep sequencing technologies are powerful tools to obtain insight into the gene expression changes underlying host responses to infectious agents. In several recent studies, these technologies have been used to characterize zebrafish infection models (Encinas *et al.*, 2010; Hegedus *et al.*, 2009; Meijer *et al.*, 2005; Ordas *et al.*, 2010; Stockhammer *et al.*, 2009, 2010; van der Sar *et al.*, 2009; Wu *et al.*, 2010). In the following section, an overview of the available platforms is given, with guidelines for their use and a protocol to isolate high-quality mRNA from zebrafish embryos for transcriptome analysis.

1. Microarray-Based Transcriptome Analysis

Commercial microarray chips for zebrafish are available from Affymetrix, Agilent Technologies, and NimbleGen. The Affymetrix GeneChip® Zebrafish Genome Array allows studying gene expression of over 14,900 zebrafish transcripts. However, the sequence information is derived from databank releases from 2003 and, thus, is not up to date. Agilent offers the Zebrafish (V3) Gene Expression Microarray 4×44K, containing 43,803 probes sourced among others from RefSeq (Release 38, November 2009), Unigene (Release 117, September 2009), and Ensembl (Release 56, September 2009), and, in addition, provides a service to order custom-designed chips. Nimblegen, which also provides custom design, claims the most comprehensive commercial design with its 385k arrays based on the Zv7 genome build. We currently use a 180k custom-made Agilent design containing 133,691 sequences derived from the Zv8 genome build (Ensembl 57, Vega 37) and the RefSeq 39 and UniGene 117 databases (Rauwerda *et al.*, 2010).

Labeling samples with fluorescent dyes can be achieved by either direct or indirect labeling reactions. In the first case, the fluorescent label is directly incorporated during cDNA synthesis and aRNA amplification or in a post-aRNA reverse transcription reaction. Indirect labeling, on the other hand, incorporates a modified nucleotide to which the fluorescent label is later attached. Although direct labeling is faster (one step vs. two steps), it is more expensive and less suited for dye swapping. Furthermore, the use of labeled nucleotides in the direct labeling procedure can lead to variations in the incorporation efficiency of different dyes because Cy-labeled dyes have lower incorporation efficiencies.

Good results were obtained for RNA derived from zebrafish embryos using the Amino Allyl Message Amp™ II aRNA amplification kit (Ambion). Amino allyl UTP is incorporated during the *in vitro* transcription reaction step, resulting in amino allyl aRNA that subsequently can be coupled to either a Cy3 or Cy5 amine-reactive dye. The kit is supplied with material for 20 reactions. However, by using only half of the supplied materials for each reaction, aRNA for up to 40 samples can be sufficiently amplified and labeled. To prevent loss of yield during the cDNA and aRNA cleanup steps, those need to be carried out as recommended by the manufacturer. Routinely, we use 500 ng of high-quality RNA as starting material and perform all

steps of the first- and second-strand cDNA synthesis as well as the aRNA synthesis using only half of the recommended reagents. If necessary, the input amount of RNA can be lowered to 200 ng without requiring an extra round of amplification. When two rounds of amplification are used, the first with UTP and the second with amino allyl UTP, RNA amounts down to 20 ng are sufficient.

The experimental design of microarray studies is very important for data interpretation and should include proper controls for each treatment. For example, in the case of a bacterial infection via injection, zebrafish embryos injected with the carrier (e.g., PBS) alone should be included to control for gene expression changes induced by the wounding response. In the case of combinations with morpholino knockdown, good controls should be included for the morpholino treatment because these could also induce immune-related responses. In our studies, we have used a standard control morpholino supplied by Genetools or mismatch morpholinos as controls (Stockhammer *et al.*, 2010; Zakrzewska *et al.*, 2010). Furthermore, for sufficient statistical power in the data analysis, the experiment should consist of three to five biological replicates, and the treatment order should be randomized. If a two-color platform, such as the Agilent microarray chip, is used, one can choose to compare samples directly to each other (competitive hybridization of two samples) or via a common reference approach (competitive hybridization of the samples vs. the common reference). Choosing a common reference approach avoids the need for a dye swap and gives greater flexibility in the subsequent analysis as all samples can be compared to each other.

2. Next-Generation Sequencing

Next-generation sequencing technologies such as Solexa (Illumina) or SOLID (Applied Biosystems) are powerful alternatives to microarray experiments and have recently been applied for transcriptome profiling studies in zebrafish (Hegedus *et al.*, 2009; Ordas *et al.*, 2010; Stockhammer *et al.*, 2010). Solexa and SOLID are able to sequence in parallel up to tens of millions of DNA molecules derived directly from mRNA (Wang *et al.*, 2009). The direct sequencing yields libraries of short (25–50 nucleotides) sequences that then need to be mapped onto the relevant genome or transcript database. Avoiding the inherent limitations of microarray-based analysis, such as a low dynamic range and a sequence-based design, deep sequencing permits detection and quantification of low-abundance mRNA and transcript isoforms. However, due to considerably lower costs and less complex data analysis, microarrays remain highly useful, especially for the analysis of larger numbers of biological samples.

Two different approaches for deep sequencing of the transcriptome are whole-transcriptome sequencing, known as RNA-Seq, and tag-based sequencing, referred to as Tag-Seq or Digital Gene Expression (DGE). In RNA-Seq methods, RNA is first sheared and converted to cDNA, or cDNA is produced first and then sheared into short fragments. In Tag-Seq or DGE, cDNA is enzymatically digested and the 3′ ends are captured on magnetic beads. Subsequently, a second enzyme is used to cut a short

fragment from the 5′ end of each captured cDNA, thus providing a library of sequence-specific tags that are further processed for sequencing. Both methods proved suitable for quantification of transcriptome changes during infection of zebrafish embryos (Ordas *et al.*, 2010).

3. RNA Isolation Protocol

RNA quality is crucial for transcriptome analysis. A good way to assess RNA quality is Lab-on-Chip analysis (Agilent Technologies). An RNA Integrity Number (RIN, quality measurement from Agilent Technologies) greater or equal to 7 is generally considered sufficient, but we prefer not to use samples with RIN values below 8. Below we provide a protocol that normally generates RNA with an RIN value between 9 and 10.

RNA Isolation Protocol for Pools of 15–20 Embryos

1. Collect embryos in a 2-mL reaction tube; remove remaining water and immediately immerse embryos in 500 μL TRIzol® reagent (Invitrogen). Alternatively, embryos can be immersed in RNA*later*® (Ambion) or snap frozen in liquid nitrogen and stored at 4 or −80 °C, respectively.
2. Homogenize embryos either by passing the embryos repeatedly through an injection needle (21G 2″, 0.8 × 50 mm) or by using a grinder, such as the MM 301 mixer mill (Retsch, 2 × 30 s at maximum frequency). In the latter case, place a metal bead (4 mm diameter, Fabory) in the tube before grinding. Transfer the homogenate sample to a new 1.5-mL tube.
3. Centrifuge for 10 min at 12,000 × *g* (4 °C) and subsequently transfer supernatant to a new tube.
4. Incubate samples for 5 min at RT.
5. Add 0.1 mL chloroform. Cap sample tubes securely and shake vigorously by hand for 15 s.
6. Incubate samples for 2–3 min at RT.
7. Centrifuge for 10 min at full speed (4 °C) in an Eppendorf centrifuge for phase separation. The mixture separates into a lower phenol chloroform phase (red), an interphase (white), and a colorless upper aqueous phase. RNA remains exclusively in the aqueous phase. Transfer the aqueous phase to a new 1.5-mL tube.
8. Add 0.25 mL of isopropyl alcohol and mix by turning the tube upside down for several times.
9. Incubate samples for 10 min at RT.
10. Centrifuge at no more than 12,000 × *g* for 10 min at 4 °C. The RNA will form a gel-like pellet that is sometimes hard to see.
11. Remove the supernatant and wash the pellet once with 0.5–1 mL of 75% ethanol, and centrifuge at 7500 × *g* for 5 min at 4 °C.
12. Remove the supernatant and air-dry the pellet for 5–10 min at RT.

13. To dissolve the RNA, incubate in 100 μL of RNase-free water for 10 min at 55 °C and vortex well.
14. To remove contaminating DNA that might interfere with subsequent applications, treat RNA samples for 20 min at 37 °C with 10 U of RNase-free DNase I (Roche Applied Science).
15. Column-purify the samples using the RNeasy MinElute Cleanup Kit (Qiagen).

Several other commercial kits for RNA isolation will also produce good results. For example, we have had good results with the Ambion RNAqueous Microkit to obtain RNA from FACS-sorted cells (Zakrzewska *et al.*, 2010). If RNA samples will also be used for microRNA analysis, the miRNeasy Mini kit (Qiagen) provides good preservation of small RNA species. For isolating RNA from individual embryos, we use a recently published method that provides sufficient high-quality mRNA for microarray analysis from single embryos (de Jong *et al.*, 2010). This method, using a combination of sample homogenization in liquid nitrogen, RNA extraction with phenol (Qiazol, Qiagen), and column purification (RNeasy MinElute Cleanup Kit, Qiagen), yields approximately 200–500 ng RNA per embryo.

C. Morpholino Knockdown of Innate Immunity Mediators

Morpholinos are the most widely used knockdown tools in zebrafish. Common practices for their use and potential pitfalls of morpholino application have been extensively reviewed (Bill *et al.*, 2009; Eisen and Smith, 2008). Morpholinos can be applied to block translation (AUG MOs) or pre-mRNA splicing (splice MOs). Due to the lack of antibody tools to check efficacy of AUG MOs, it may be preferable to use splice MOs where the effects can be checked by reverse transcription PCR. Injection of morpholinos into zebrafish embryos at the one- to two-cell stage can result in a variable period of transient knockdown. For example, MyD88 and TNFR MOs have been used up to 5–8 days to study gut immune responses and *M. marinum* infection, whereas other MOs are less effective or toxic at higher doses (Bates *et al.*, 2007; Clay *et al.*, 2008).

As shown in Table II, morpholino knockdown of the Spi1/Pu.1 transcription factor has been frequently used for infection studies (Brannon *et al.*, 2009; Clatworthy *et al.*, 2009; Clay *et al.*, 2007; Prajsnar *et al.*, 2008; Wiles *et al.*, 2009; Zakrzewska *et al.*, 2010). Knockdown of this transcription factor results in embryos that lack macrophages and show a major reduction of neutrophils during the first days of development (Fig. 3) (Rhodes *et al.*, 2005; Su *et al.*, 2007). Spi1/Pu.1 morphants showed increased susceptibility to *Pseudomonas aeruginosa* and *Staphylococcus aureus* infections (Brannon *et al.*, 2009; Clatworthy *et al.*, 2009; Prajsnar *et al.*, 2008). In addition, Spi1 knockdown studies demonstrated that macrophages play an essential role in tissue dissemination of *M. marinum* infection (Clay *et al.*, 2007). A dual microarray approach, in which genes downregulated by Spi1/Pu.1 morpholino knockdown were compared with genes enriched in FACS-sorted myeloid cells from *spi1:GFP* transgenic embryos, was used in our laboratory to identify the putative

Table II
Overview of innate immunity mediators studied by morpholino knockdown in zebrafish embryos

Genes	Functions	Conclusion from knockdown experiments	References
crfb family	Cytokine receptor family member b	Different receptor complexes required for signaling of IFN-γ and IFN-φ interferons	Aggad *et al.* (2010)
cftr	Cystic fibrosis transmembrane conductance regulator	Required for control of *Pseudomonas aeruginosa* infection	Phennicie *et al.* (2010)
csf3r	Granulocyte colony-stimulating factor receptor	Required for primitive and definitive myelopoiesis, early myeloid cell migration, and LPS-induced emergency myelopoiesis	Liongue *et al.* (2009)
cxcr3.2	CXCL chemokine receptor, homologous to human CXCR3/CXCR5	Required for macrophage migration to bacterial infection sites	Zakrzewska *et al.* (2010)
duox	Member of the NADPH-oxidase family	Required to control enteric *S. typhimurium* infection	Flores *et al.* (2010)
gprk2	NFκB signaling regulator	Required for *Escherichia coli*–induced *tnfa* and *il1b* expression	Valanne *et al.* (2010)
ifng1-1,1-2	IFN-γ family members	Required for control of *E. coli* and *Yersinia ruckeri* infections Signals through specific crfb receptor complexes	Sieger *et al.* (2009) Aggad *et al.* (2010)
irf8	Interferon regulatory transcription factor 8	Regulation of macrophage versus neutrophil cell fate during primitive myelopoiesis	Li *et al.* (2010)
ita4h	Leukotriene A_4 hydrolase	Required for proinflammatory leukotriene production. Knockdown results in increased anti-inflammatory lipoxin production and susceptibility to *Mycobacterium marinum* infection	Tobin *et al.* (2010)
mmp9	Matrix metalloproteinase family member	Required for recruitment of macrophages during mycobacterial granuloma formation	Volkman *et al.* (2010)
myd88	Adaptor molecule for TLRs and IL1R	Required for control of *S. typhimurium* Ra infection	van der Sar *et al.* (2006)
		Myd88-dependent induction of *il1b*, *mmp9*, and *irak3* during *S. typhimurium* infection	Stockhammer *et al.* (2009), Liu *et al.* (2010)
		Myd88-dependent induction of *il1b* in response to peptidoglycans (PGNs) and lipoteichoic acid (LTA)	Cheesman *et al.* (2010)
		Required for gut responses to endogenous microbiota	Bates *et al.* (2007)

(Continued)

Table II *(Continued)*

Genes	Functions	Conclusion from knockdown experiments	References
pglyrp5	Peptidoglycan recognition protein	Required for defense against *Salmonella enterica* and *Bacillus subtilis* infections	Li *et al.* (2007)
spi1 (*pu.1*)	Hematopoietic transcription factor	Myeloid cell depletion	Rhodes *et al.* (2005), Su *et al.* (2007)
		Required for control of *M. marinum*, *E. coli*, *P. aeruginosa*, *S. typhimurium*, and *Staphylococcus aureus* infections	Clay *et al.* (2007), Prajsnar *et al.* (2008), Brannon *et al.* (2009), Clatworthy *et al.* (2009), Wiles *et al.* (2009)
		Required for expression of a myeloid-specific gene set	Zakrzewska *et al.* (2010)
tlr4a/b	TLR family member, LPS receptor in mammals	Not required for LPS recognition	Sepulcre *et al.* (2009)
tlr5	TLR family member, flagellin receptor in mammals	Required for flagellin-induced *mmp9*, *cxcl-C1c*, *irak3*, *il8*, and *il1b* expression	Stockhammer *et al.* (2009)
tnfrsf1a	Tumor necrosis factor receptor 1	Required for intestinal immune cell homeostasis and intestinal inflammation in response to LPS	Bates *et al.* (2007)
		Required for control of *M. marinum* infection	Clay *et al.* (2008)
traf6	Signaling intermediate in TNFR and TLR signaling	Required for induction and repression of specific sets of immune response genes	Stockhammer *et al.* (2010)

targets of Spi1-directed innate immunity. By morpholino knockdown, one of the Spi1-dependent macrophage markers identified in this approach, the chemokine receptor gene *cxcr3.2*, was shown to be involved in macrophage migration to the site of bacterial infection (Zakrzewska *et al.*, 2010).

MyD88 is a pivotal signaling component of the innate immune response, serving as an adaptor for the interleukin 1 receptor and the majority of TLRs (Takeda and Akira, 2007). The role of MyD88 during bacterial infection in zebrafish embryos has been demonstrated by conducting morpholino knockdown studies with *S. typhimurium* challenge (van der Sar *et al.*, 2003). The induction levels of *mmp9*, *il1b*, and *irak3* expression were significantly reduced in the MyD88 morphants, whereas no changes were observed for *ifnphi1* or *il8* expression, indicating that both MyD88-dependent and MyD88-independent signaling pathways are involved in the innate immune response to *S. typhimurium* infection (Stockhammer *et al.*, 2009). Traf6, which functions downstream of MyD88 and in TNF receptor signaling, was also studied by morpholino knockdown. Although higher concentrations of Traf6 morpholino caused developmental aberrations, the role of Traf6 in the response to *S. typhimurium*

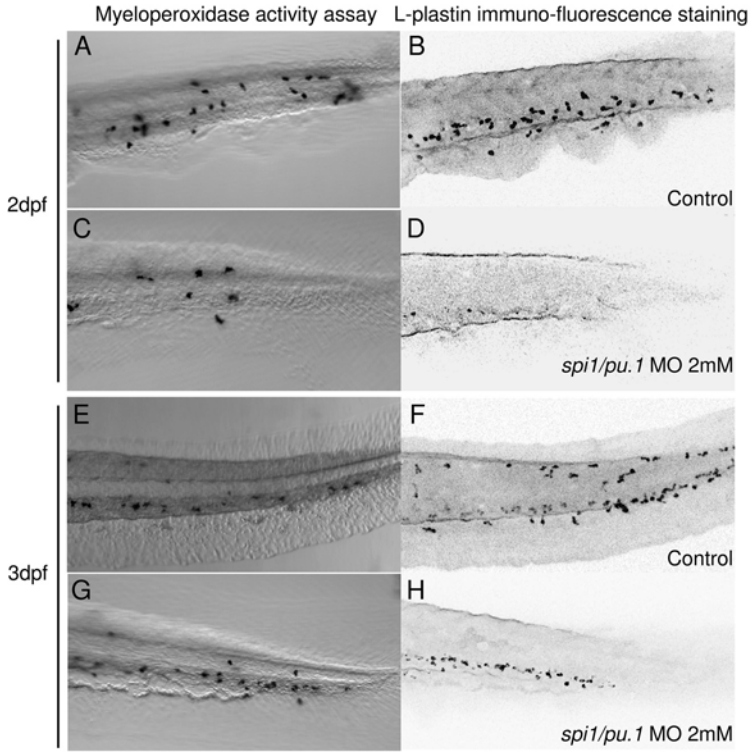

Fig. 3 Reduction of myeloid cell development by knockdown of the Spi1 transcription factor. A combination of myeloperoxidase (Mpx) activity assay and L-plastin immunofluorescence staining is used for the detection of neutrophils and macrophages in *spi1* morpholino-injected (MO) and control embryos. Details of the tail region are shown. (A, C, E, and G) Bright-field images of Mpx-activity stained neutrophils in wild-type embryos (A and E) and spi1 morphants (C and G). (B, D, F, and H) Confocal Z-stack images of L-plastin immunofluorescence staining applied on the same embryos to visualize the macrophage population. L-Plastin staining detected with Alexa 568-conjugated secondary antibody is shown in black. Although L-plastin is also present in neutrophils, the Alexa 568 fluorescence signal is not visible in these cells due to interference of the precipitate of the Mpx staining. Knockdown of spi1/pu.*1* significantly reduced the amount of neutrophils (C) and completely abolished macrophages (D) at 2 dpf. Recovery of the neutrophils was detected at 3 dpf (G). In contrast, the number of macrophages was still significantly reduced (H) and these cells appeared immature in morphology compared to the macrophages in the control (F). The *spi1* MO (Rhodes *et al.*, 2005) can be used at high doses (at least up to 2 mM with injection of 1 nL) without causing any visible developmental defects other than the reduction of myeloid cells. The MO concentration can be titrated to manipulate the ratio between macrophages and neutrophils. At lower doses of MO, neutrophil differentiation is already restored to wild-type levels at 2 dpf, while macrophage development is still strongly reduced.

could be studied by titrating the morpholino. The combined use of microarray analysis and whole-transcriptome deep sequencing demonstrated the dynamic role of Traf6 as a positive and negative regulator in the innate immune response of 1-day-old embryos (Stockhammer *et al.*, 2010). TNF signaling was also shown to play an

important role in the innate immune response of zebrafish embryos (Clay *et al.*, 2008). Morpholino knockdown of the TNF receptor 1 gene, *tnfrsf1a* (*tnfr1*), accelerated intracellular *M. marinum* growth and granuloma formation, followed by necrotic death of macrophages and granuloma breakdown, which provided direct evidence that TNF signaling is protective during the early stages of mycobacterial infection in the absence of adaptive immunity. In a subsequent study, TNF production levels during *M. marinum* infection were shown to depend on the balance between proinflammatory and anti-inflammatory lipid mediators (Tobin *et al.*, 2010).

Morpholino technology was also used to investigate signaling by interferon gamma (IFN-γ) and virus-induced interferons (IFN-φ) (Aggad *et al.*, 2010; Sieger *et al.*, 2009). Partially redundant functions were found for the *ifng1-1* and *ifng1-2* genes in mediating resistance against *E. coli* and *Yersinia ruckeri* infections, whereas raising IFN-γ levels sensitized embryos against bacterial infection, indicating the necessity of a tight control of IFN-γ levels (Sieger *et al.*, 2009). Morpholino knockdown of the NADPH oxidase family member, dual oxidase (*duox*), required for production of reactive oxygen species, led to an impaired capacity of zebrafish larvae to control enteric *S. typhimurium* infection (Flores *et al.*, 2010). Knockdown of the cystic fibrosis transmembrane conductance regulator (*cftr*) gene also dampened the respiratory burst in zebrafish embryos and led to an increased bacterial burden during *P. aeruginosa* infection (Phennicie *et al.*, 2010). A complete overview of innate immune response genes studied by morpholino knockdown in zebrafish embryos is given in Table II.

V. Conclusions

Zebrafish embryos provide an ideal vertebrate model to study infectious diseases due to their optical clarity, large number of embryos, fast development, and high similarity with human immunity counterparts. Many different infection models and techniques have been established to address the functions of key factors and crucial mechanisms in the complex host–pathogen interaction, which has accompanied the entire history of human evolution. In this chapter, we have summarized the current knowledge on zebrafish innate immune cells and described the available assays for observation and isolation of distinct cell populations, and local and systemic infection methods in zebrafish embryos. This overview shows that the zebrafish model is highly suitable to study the many challenging problems in the understanding of the innate immune system. For example, it will be possible to link the great wealth in transcriptomic data obtained from RNA-microarray-based transcriptome profiling and novel deep sequencing approaches with cellular imaging technologies. Such cellular imaging technologies are possible even at the scale of single molecules (Schaaf *et al.*, 2009), and, therefore, this integration can lead to insights into dynamic molecular processes involved in cellular recognition. Furthermore, it will be possible to link these molecular insights to functions in various differentiation processes of immune cells. These differentiation processes that are dependent on highly

dynamic communication between various cell types are currently still poorly understood because they are difficult to study in cell culture models. This means that in future zebrafish research, there will be an increased need to employ methods that are commonly used in cell culture studies, such as high-throughput genetic knockdown studies in combination with pharmaceutical approaches to analyze cell signaling components functionally. For such approaches, an increased availability of antibody tools, knockout lines, and additional transgenic reporters is still needed. These tools can be applied in automated injection and high-throughput detection systems making the zebrafish infection models a powerful tool for large-scale drug screening. This will significantly improve our understanding of infectious diseases in an *in vivo* setting, and by comparisons with data from cell culture and rodent test systems will have many clinical implications. In fact, the approaches described in this chapter are already used for the analysis of other disease models in zebrafish (Mione *et al.*, 2009). Several direct applications of these technologies for analysis of disease processes in which the immune system plays an important role, such as cancer, are currently underway in our department (Snaar-Jagalska, 2009).

Acknowledgments

CC, ELB, and MvdV are supported by the Smart Mix Programme of the Netherlands Ministry of Economic Affairs and the Ministry of Education, Culture and Science. ZK is supported by the Higher Education Commission of Pakistan. OWS is supported by the European Commission 7th framework project ZF-HEALTH (HEALTH-F4-2010-242048). AZ is supported by a Horizon grant of the Netherlands Genomics Initiative. The work in our laboratory was additionally supported by the European Commission 6th framework projects ZF-MODELS (LSHG-CT-2003-503496) and ZF-TOOLS (LSHG-2006-037220).

References

Aggad, D., Stein, C., Sieger, D., Mazel, M., Boudinot, P., Herbomel, P., Levraud, J. P., Lutfalla, G., and Leptin, M. (2010). In vivo analysis of Ifn-{gamma}1 and Ifn-{gamma}2 signaling in zebrafish. *J. Immunol.* **185**, 6774–6782.

Allen, J. P., and Neely, M. N. (2010). Trolling for the ideal model host: zebrafish take the bait. *Future Microbiol.* **5**, 563–569.

Amacher, S. L. (2008). Emerging gene knockout technology in zebrafish: zinc-finger nucleases. *Brief Funct. Genomic Proteomic* **7**, 460–464.

Balla, K. M., Lugo-Villarino, G., Spitsbergen, J. M., Stachura, D. L., Hu, Y., Banuelos, K., Romo-Fewell, O., Aroian, R. V., and Traver, D. (2010). Eosinophils in the zebrafish: prospective isolation, characterization, and eosinophilia induction by helminth determinants. *Blood* **116**, 3944–3954.

Bates, J. M., Akerlund, J., Mittge, E., and Guillemin, K. (2007). Intestinal alkaline phosphatase detoxifies lipopolysaccharide and prevents inflammation in zebrafish in response to the gut microbiota. *Cell Host Microbe* **2**, 371–382.

Bennett, C. M., Kanki, J. P., Rhodes, J., Liu, T. X., Paw, B. H., Kieran, M. W., Langenau, D. M., Delahaye-Brown, A., Zon, L. I., Fleming, M. D., and Look, A. T. (2001). Myelopoiesis in the zebrafish. *Danio rerio. Blood* **98**, 643–651.

Bertrand, J. Y., Cisson, J. L., Stachura, D. L., and Traver, D. (2010). Notch signaling distinguishes 2 waves of definitive hematopoiesis in the zebrafish embryo. *Blood* **115**, 2777–2783.

Bertrand, J. Y., Kim, A. D., Violette, E. P., Stachura, D. L., Cisson, J. L., and Traver, D. (2007). Definitive hematopoiesis initiates through a committed erythromyeloid progenitor in the zebrafish embryo. *Development* **134**, 4147–4156.

Bertrand, J. Y., and Traver, D. (2009). Hematopoietic cell development in the zebrafish embryo. *Curr. Opin. Hematol.* **16**, 243–248.

Bill, B. R., Petzold, A. M., Clark, K. J., Schimmenti, L. A., and Ekker, S. C. (2009). A primer for morpholino use in zebrafish. *Zebrafish* **6**, 69–77.

Boisset, J. C., van Cappellen, W., Andrieu-Soler, C., Galjart, N., Dzierzak, E., and Robin, C. (2010). In vivo imaging of haematopoietic cells emerging from the mouse aortic endothelium. *Nature* **464**, 116–120.

Brannon, M. K., Davis, J. M., Mathias, J. R., Hall, C. J., Emerson, J. C., Crosier, P. S., Huttenlocher, A., Ramakrishnan, L., and Moskowitz, S. M. (2009). Pseudomonas aeruginosa type III secretion system interacts with phagocytes to modulate systemic infection of zebrafish embryos. *Cell. Microbiol* **11**, 755–768.

Carvalho, R., de Sonneville, J., Stockhammer, O. W., Savage, N. D., Veneman, W. J., Ottenhoff, T. H., Dirks, R. P., Meijer, A. H., and Spaink, H. P. (2011). A high-throughput screen for tuberculosis progression. *PLoS One* **6**, e16779.

Cheesman, S. E., Neal, J. T., Mittge, E., Seredick, B. M., and Guillemin, K. (2010). Microbes and Health Sackler Colloquium: epithelial cell proliferation in the developing zebrafish intestine is regulated by the Wnt pathway and microbial signaling via Myd88. *Proc. Natl. Acad. Sci. U.S.A.* **108**(Suppl 1), 4570–4577.

Clatworthy, A. E., Lee, J. S., Leibman, M., Kostun, Z., Davidson, A. J., and Hung, D. T. (2009). *Pseudomonas aeruginosa* infection of zebrafish involves both host and pathogen determinants. *Infect Immun.* **77**, 1293–1303.

Clay, H., Davis, J. M., Beery, D., Huttenlocher, A., Lyons, S. E., and Ramakrishnan, L. (2007). Dichotomous role of the macrophage in early *Mycobacterium marinum* infection of the zebrafish. *Cell Host Microbe* **2**, 29–39.

Clay, H., and Ramakrishnan, L. (2005). Multiplex fluorescent in situ hybridization in zebrafish embryos using tyramide signal amplification. *Zebrafish* **2**, 105–111.

Clay, H., Volkman, H. E., and Ramakrishnan, L. (2008). Tumor necrosis factor signaling mediates resistance to mycobacteria by inhibiting bacterial growth and macrophage death. *Immunity* **29**, 283–294.

Coban, C., Ishii, K. J., and Akira, S. (2009). Immune interventions of human diseases through toll-like receptors. *Adv. Exp. Med. Biol.* **655**, 63–80.

Cosma, C. L., Swaim, L. E., Volkman, H., Ramakrishnan, L., and Davis, J. M. (2006). Zebrafish and frog models of *Mycobacterium marinum* infection. *Curr. Protoc. Microbiol.* Chapter 10, Unit 10B.2.

Covassin, L., Amigo, J. D., Suzuki, K., Teplyuk, V., Straubhaar, J., and Lawson, N. D. (2006). Global analysis of hematopoietic and vascular endothelial gene expression by tissue specific microarray profiling in zebrafish. *Dev. Biol.* **299**, 551–562.

Davidson, A. J., and Zon, L. I. (2004). The 'definitive' (and 'primitive') guide to zebrafish hematopoiesis. *Oncogene* **23**, 7233–7246.

Davis, J. M., Clay, H., Lewis, J. L., Ghori, N., Herbomel, P., and Ramakrishnan, L. (2002). Real-time visualization of mycobacterium–macrophage interactions leading to initiation of granuloma formation in zebrafish embryos. *Immunity* **17**, 693–702.

Davis, J. M., Haake, D. A., and Ramakrishnan, L. (2009). *Leptospira interrogans* stably infects zebrafish embryos, altering phagocyte behavior and homing to specific tissues. *PLoS Negl. Trop. Dis.* **3**, e463.

Davis, J. M., and Ramakrishnan, L. (2009). The role of the granuloma in expansion and dissemination of early tuberculous infection. *Cell* **136**, 37–49.

de Jong, J. L., Davidson, A. J., Wang, Y., Palis, J., Opara, P., Pugach, E., Daley, G. Q., and Zon, L. I. (2010). Interaction of retinoic acid and scl controls primitive blood development. *Blood* **116**, 201–209.

Del Bene, F., Wyart, C., Robles, E., Tran, A., Looger, L., Scott, E. K., Isacoff, E. Y., and Baier, H. (2010). Filtering of visual information in the tectum by an identified neural circuit. *Science* **330**, 669–673.

Eisen, J. S., and Smith, J. C. (2008). Controlling morpholino experiments: don't stop making antisense. *Development* **135**, 1735–1743.

Ellett, F., Pase, L., Hayman, J. W., Andrianopoulos, A., and Lieschke, G. J. (2010). mpeg1 promoter transgenes direct macrophage-lineage expression in zebrafish. *Blood* **117**, e49–e56.

Encinas, P., Rodriguez-Milla, M. A., Novoa, B., Estepa, A., Figueras, A., and Coll, J. (2010). Zebrafish fin immune responses during high mortality infections with viral haemorrhagic septicemia rhabdovirus. A proteomic and transcriptomic approach. *BMC Genomics* **11**, 518.

Flores, M. V., Crawford, K. C., Pullin, L. M., Hall, C. J., Crosier, K. E., and Crosier, P. S. (2010). Dual oxidase in the intestinal epithelium of zebrafish larvae has anti-bacterial properties. *Biochem. Biophys. Res. Commun.* **400**, 164–168.

Gray, C., Loynes, C. A., Whyte, M. K., Crossman, D. C., Renshaw, S. A., and Chico, T. J. (2011). Simultaneous intravital imaging of macrophage and neutrophil behaviour during inflammation using a novel transgenic zebrafish. *Thromb. Haemost* **105**, 811–819.

Gutzman, J. H., and Sive, H. (2009). Zebrafish brain ventricle injection. *J. Vis. Exp.* **26**, http://www.jove.com/details.php?id=1218, doi: 10.3791/1218.

Haffter, P., and Nusslein-Volhard, C. (1996). Large scale genetics in a small vertebrate, the zebrafish. *Int. J. Dev. Biol.* **40**, 221–227.

Hall, C., Flores, M. V., Crosier, K., and Crosier, P. (2009). Live cell imaging of zebrafish leukocytes. *Methods Mol. Biol.* **546**, 255–271.

Hall, C., Flores, M. V., Storm, T., Crosier, K., and Crosier, P. (2007). The zebrafish lysozyme C promoter drives myeloid-specific expression in transgenic fish. *BMC Dev. Biol.* **7**, 42.

Halpern, M. E., Rhee, J., Goll, M. G., Akitake, C. M., Parsons, M., and Leach, S. D. (2008). Gal4/UAS transgenic tools and their application to zebrafish. *Zebrafish* **5**, 97–110.

Hegedus, Z., Zakrzewska, A., Agoston, V. C., Ordas, A., Racz, P., Mink, M., Spaink, H. P., and Meijer, A. H. (2009). Deep sequencing of the zebrafish transcriptome response to mycobacterium infection. *Mol. Immunol.* **46**, 2918–2930.

Herbomel, P., and Levraud, J. P. (2005). Imaging early macrophage differentiation, migration, and behaviors in live zebrafish embryos. *Methods Mol. Med.* **105**, 199–214.

Herbomel, P., Thisse, B., and Thisse, C. (1999). Ontogeny and behaviour of early macrophages in the zebrafish embryo. *Development* **126**, 3735–3745.

Herbomel, P., Thisse, B., and Thisse, C. (2001). Zebrafish early macrophages colonize cephalic mesenchyme and developing brain, retina, and epidermis through a M-CSF receptor-dependent invasive process. *Dev. Biol.* **238**, 274–288.

Hermann, A. C., Millard, P. J., Blake, S. L., and Kim, C. H. (2004). Development of a respiratory burst assay using zebrafish kidneys and embryos. *J. Immunol. Methods* **292**, 119–129.

Hsu, K., Traver, D., Kutok, J. L., Hagen, A., Liu, T. X., Paw, B. H., Rhodes, J., Berman, J. N., Zon, L. I., Kanki, J. P., and Look, A. T. (2004). The pu.1 promoter drives myeloid gene expression in zebrafish. *Blood* **104**, 1291–1297.

Jault, C., Pichon, L., and Chluba, J. (2004). Toll-like receptor gene family and TIR-domain adapters in *Danio rerio*. *Mol. Immunol.* **40**, 759–771.

Kanther, M., and Rawls, J. F. (2010). Host–microbe interactions in the developing zebrafish. *Curr. Opin. Immunol.* **22**, 10–19.

Kimmel, C. B., Ballard, W. W., Kimmel, S. R., Ullmann, B., and Schilling, T. F. (1995). Stages of embryonic development of the zebrafish. *Dev. Dyn.* **203**, 253–310.

Kissa, K., and Herbomel, P. (2010). Blood stem cells emerge from aortic endothelium by a novel type of cell transition. *Nature* **464**, 112–115.

Lam, S. H., Chua, H. L., Gong, Z., Lam, T. J., and Sin, Y. M. (2004). Development and maturation of the immune system in zebrafish, *Danio rerio*: a gene expression profiling, in situ hybridization and immunological study. *Dev. Comp. Immunol.* **28**, 9–28.

Le Guyader, D., Redd, M. J., Colucci-Guyon, E., Murayama, E., Kissa, K., Briolat, V., Mordelet, E., Zapata, A., Shinomiya, H., and Herbomel, P. (2008). Origins and unconventional behavior of neutrophils in developing zebrafish. *Blood* **111**, 132–141.

Lepiller, S., Laurens, V., Bouchot, A., Herbomel, P., Solary, E., and Chluba, J. (2007). Imaging of nitric oxide in a living vertebrate using a diamino-fluorescein probe. *Free Radic. Biol. Med.* **43**, 619–627.

Lesley, R., and Ramakrishnan, L. (2008). Insights into early mycobacterial pathogenesis from the zebrafish. *Curr. Opin. Microbiol.* **11**, 277–283.

Levraud, J. P., Colucci-Guyon, E., Redd, M. J., Lutfalla, G., and Herbomel, P. (2008). In vivo analysis of zebrafish innate immunity. *Methods Mol. Biol.* **415**, 337–363.

Levraud, J. P., Disson, O., Kissa, K., Bonne, I., Cossart, P., Herbomel, P., and Lecuit, M. (2009). Real-time observation of *Listeria monocytogenes*–phagocyte interactions in living zebrafish larvae. *Infect Immun.* **77**, 3651–3660.

Li, L., Jin, H., Xu, J., Shi, Y., and Wen, Z. (2010). Irf8 regulates macrophage versus neutrophil fate during zebrafish primitive myelopoiesis. *Blood* **117**, 1359–1369.

Li, X., Wang, S., Qi, J., Echtenkamp, S. F., Chatterjee, R., Wang, M., Boons, G. J., Dziarski, R., and Gupta, D. (2007). Zebrafish peptidoglycan recognition proteins are bactericidal amidases essential for defense against bacterial infections. *Immunity* **27**, 518–529.

Lieschke, G. J., Oates, A. C., Crowhurst, M. O., Ward, A. C., and Layton, J. E. (2001). Morphologic and functional characterization of granulocytes and macrophages in embryonic and adult zebrafish. *Blood* **98**, 3087–3096.

Liongue, C., Hall, C. J., O'Connell, B. A., Crosier, P., and Ward, A. C. (2009). Zebrafish granulocyte colony-stimulating factor receptor signaling promotes myelopoiesis and myeloid cell migration. *Blood* **113**, 2535–2546.

Liu, Y., Li, M., Fan, S., Lin, Y., Lin, B., Luo, F., Zhang, C., Chen, S., Li, Y., and Xu, A. (2010). A unique feature of Toll/IL-1 receptor domain-containing adaptor protein is partially responsible for lipopolysaccharide insensitivity in zebrafish with a highly conserved function of Myd88. *J. Immunol.* **185**, 3391–3400.

Lugo-Villarino, G., Balla, K. M., Stachura, D. L., Banuelos, K., Werneck, M. B., and Traver, D. (2010). Identification of dendritic antigen-presenting cells in the zebrafish. *Proc. Natl. Acad. Sci. U. S. A.* **107**, 15850–15855.

Mathias, J. R., Dodd, M. E., Walters, K. B., Rhodes, J., Kanki, J. P., Look, A. T., and Huttenlocher, A. (2007). Live imaging of chronic inflammation caused by mutation of zebrafish Hai1. *J. Cell Sci.* **120**, 3372–3383.

Mathias, J. R., Perrin, B. J., Liu, T. X., Kanki, J., Look, A. T., and Huttenlocher, A. (2006). Resolution of inflammation by retrograde chemotaxis of neutrophils in transgenic zebrafish. *J. Leukoc. Biol.* **80**, 1281–1288.

Mathias, J. R., Walters, K. B., and Huttenlocher, A. (2009). Neutrophil motility in vivo using zebrafish. *Methods Mol. Biol.* **571**, 151–166.

Meeker, N. D., and Trede, N. S. (2008). Immunology and zebrafish: spawning new models of human disease. *Dev. Comp. Immunol.* **32**, 745–757.

Meijer, A. H., Gabby Krens, S. F., Medina Rodriguez, I. A., He, S., Bitter, W., Ewa Snaar-Jagalska, B., and Spaink, H. P. (2004). Expression analysis of the Toll-like receptor and TIR domain adaptor families of zebrafish. *Mol. Immunol.* **40**, 773–783.

Meijer, A. H., and Spaink, H. P. (2011). Host–pathogen interactions made transparent with the zebrafish model. *Curr Drug Targets.* **12**, 1000–1017.

Meijer, A. H., van der Sar, A. M., Cunha, C., Lamers, G. E., Laplante, M. A., Kikuta, H., Bitter, W., Becker, T. S., and Spaink, H. P. (2008). Identification and real-time imaging of a myc-expressing neutrophil population involved in inflammation and mycobacterial granuloma formation in zebrafish. *Dev. Comp. Immunol.* **32**, 36–49.

Meijer, A. H., Verbeek, F. J., Salas-Vidal, E., Corredor-Adamez, M., Bussman, J., van der Sar, A. M., Otto, G. W., Geisler, R., and Spaink, H. P. (2005). Transcriptome profiling of adult zebrafish at the late stage of chronic tuberculosis due to *Mycobacterium marinum* infection. *Mol. Immunol.* **42**, 1185–1203.

Mione, M., Meijer, A. H., Snaar-Jagalska, B. E., Spaink, H. P., and Trede, N. S. (2009). Disease modeling in zebrafish: cancer and immune responses – a report on a workshop held in Spoleto, Italy, July 20-22, 2009. *Zebrafish* **6**, 445–451.

Mogensen, T. H. (2009). Pathogen recognition and inflammatory signaling in innate immune defenses. *Clin. Microbiol. Rev.* **22**, 240–273 (Table of Contents).

Murayama, E., Kissa, K., Zapata, A., Mordelet, E., Briolat, V., Lin, H. F., Handin, R. I., and Herbomel, P. (2006). Tracing hematopoietic precursor migration to successive hematopoietic organs during zebrafish development. *Immunity* **25**, 963–975.

Nasevicius, A., and Ekker, S. C. (2000). Effective targeted gene 'knockdown' in zebrafish. *Nat. Genet.* **26**, 216–220.

Ordas, A., Hegedus, Z., Henkel, C. V., Stockhammer, O. W., Butler, D., Jansen, H. J., Racz, P., Mink, M., Spaink, H. P., and Meijer, A. H. (2010). Deep sequencing of the innate immune transcriptomic response of zebrafish embryos to *Salmonella* infection. *Fish Shellfish Immunol.* , Sep. 8. [Epub ahead of print] doi:10.1016/j.fsi.2010.08.022.

Peri, F., and Nusslein-Volhard, C. (2008). Live imaging of neuronal degradation by microglia reveals a role for v0-ATPase a1 in phagosomal fusion in vivo. *Cell* **133**, 916–927.

Phennicie, R. T., Sullivan, M. J., Singer, J. T., Yoder, J. A., and Kim, C. H. (2010). Specific resistance to *Pseudomonas aeruginosa* infection in zebrafish is mediated by the cystic fibrosis transmembrane conductance regulator. *Infect. Immun.* **78**, 4542–4550.

Prajsnar, T. K., Cunliffe, V. T., Foster, S. J., and Renshaw, S. A. (2008). A novel vertebrate model of *Staphylococcus aureus* infection reveals phagocyte-dependent resistance of zebrafish to non-host specialized pathogens. *Cell. Microbiol.* **10**, 2312–2325.

Rauwerda, H., de Jong, M., de Leeuw, W. C., Spaink, H. P., and Breit, T. M. (2010). Integrating heterogeneous sequence information for transcriptome-wide microarray design; a zebrafish example. *BMC Res. Notes* **3**, 192.

Redd, M. J., Kelly, G., Dunn, G., Way, M., and Martin, P. (2006). Imaging macrophage chemotaxis in vivo: studies of microtubule function in zebrafish wound inflammation. *Cell Motil. Cytoskeleton* **63**, 415–422.

Renshaw, S. A., Loynes, C. A., Trushell, D. M., Elworthy, S., Ingham, P. W., and Whyte, M. K. (2006). A transgenic zebrafish model of neutrophilic inflammation. *Blood* **108**, 3976–3978.

Rhodes, J., Hagen, A., Hsu, K., Deng, M., Liu, T. X., Look, A. T., and Kanki, J. P. (2005). Interplay of pu.1 and gata1 determines myelo-erythroid progenitor cell fate in zebrafish. *Dev. Cell* **8**, 97–108.

Russell, D. G. (2007). Who puts the tubercle in tuberculosis? *Nat. Rev. Microbiol.* **5**, 39–47.

Schaaf, M. J., Koopmans, W. J., Meckel, T., van Noort, J., Snaar-Jagalska, B. E., Schmidt, T. S., and Spaink, H. P. (2009). Single-molecule microscopy reveals membrane microdomain organization of cells in a living vertebrate. *Biophys. J.* **97**, 1206–1214.

Sepulcre, M. P., Alcaraz-Perez, F., Lopez-Munoz, A., Roca, F. J., Meseguer, J., Cayuela, M. L., and Mulero, V. (2009). Evolution of lipopolysaccharide (LPS) recognition and signaling: fish TLR4 does not recognize LPS and negatively regulates NF-kappaB activation. *J. Immunol.* **182**, 1836–1845.

Sieger, D., Stein, C., Neifer, D., van der Sar, A. M., and Leptin, M. (2009). The role of gamma interferon in innate immunity in the zebrafish embryo. *Dis. Model Mech.* **2**, 571–581.

Snaar-Jagalska, B. E. (2009). ZF-CANCER: developing high-throughput bioassays for human cancers in zebrafish. *Zebrafish* **6**, 441–443.

Stein, C., Caccamo, M., Laird, G., and Leptin, M. (2007). Conservation and divergence of gene families encoding components of innate immune response systems in zebrafish. *Genome Biol.* **8**, R251.

Stockhammer, O. W., Rauwerda, H., Wittink, F. R., Breit, T. M., Meijer, A. H., and Spaink, H. P. (2010). Transcriptome analysis of Traf6 function in the innate immune response of zebrafish embryos. *Mol. Immunol.* **48**, 179–190.

Stockhammer, O. W., Zakrzewska, A., Hegedus, Z., Spaink, H. P., and Meijer, A. H. (2009). Transcriptome profiling and functional analyses of the zebrafish embryonic innate immune response to *Salmonella* infection. *J. Immunol.* **182**, 5641–5653.

Stoop, E. M., Schipper, T., Huber, S. R., Nezhinsky, A. E., Verbeek, F. J., Gurcha, S. S., Besra, G. S., Vandenbroucke-Grauls, C. M., Bitter, W., and van der Sar, A. M. (2011). Zebrafish embryo screen for mycobacterial genes involved in granuloma formation reveals a novel ESX-1 component. *Dis. Model Mech.* **4**, 526–536.

Su, F., Juarez, M. A., Cooke, C. L., Lapointe, L., Shavit, J. A., Yamaoka, J. S., and Lyons, S. E. (2007). Differential regulation of primitive myelopoiesis in the zebrafish by Spi-1/Pu.1 and C/ebp1. *Zebrafish* **4**, 187–199.

Sullivan, C., and Kim, C. H. (2008). Zebrafish as a model for infectious disease and immune function. *Fish Shellfish Immunol.* **25**, 341–350.

Suster, M. L., Kikuta, H., Urasaki, A., Asakawa, K., and Kawakami, K. (2009). Transgenesis in zebrafish with the tol2 transposon system. *Methods Mol. Biol.* **561**, 41–63.

Swaim, L. E., Connolly, L. E., Volkman, H. E., Humbert, O., Born, D. E., and Ramakrishnan, L. (2006). *Mycobacterium marinum* infection of adult zebrafish causes caseating granulomatous tuberculosis and is moderated by adaptive immunity. *Infect Immun.* **74**, 6108–6117.

Takeda, K., and Akira, S. (2007). Toll-like receptors. *Curr. Protoc. Immunol.* Chapter 14, Unit 14.12.

Tobin, D. M., and Ramakrishnan, L. (2008). Comparative pathogenesis of *Mycobacterium marinum* and *Mycobacterium tuberculosis*. *Cell. Microbiol* **10**, 1027–1039.

Tobin, D. M., Vary Jr., J. C., Ray, J. P., Walsh, G. S., Dunstan, S. J., Bang, N. D., Hagge, D. A., Khadge, S., King, M. C., Hawn, T. R., Moens, C. B., and Ramakrishnan, L. (2010). The lta4h locus modulates susceptibility to mycobacterial infection in zebrafish and humans. *Cell* **140**, 717–730.

Traver, D., Herbomel, P., Patton, E. E., Murphey, R. D., Yoder, J. A., Litman, G. W., Catic, A., Amemiya, C. T., Zon, L. I., and Trede, N. S. (2003). The zebrafish as a model organism to study development of the immune system. *Adv. Immunol.* **81**, 253–330.

Trede, N. S., Langenau, D. M., Traver, D., Look, A. T., and Zon, L. I. (2004). The use of zebrafish to understand immunity. *Immunity* **20**, 367–379.

Valanne, S., Myllymaki, H., Kallio, J., Schmid, M. R., Kleino, A., Murumagi, A., Airaksinen, L., Kotipelto, T., Kaustio, M., Ulvila, J., Esfahani, S. S., Engstrom, Y., Silvennoinen, O., Hultmark, D., Parikka, M., and Ramet, M. (2010). Genome-wide RNA interference in *Drosophila* cells identifies G protein-coupled receptor kinase 2 as a conserved regulator of NF-kappaB signaling. *J. Immunol.* **184**, 6188–6198.

van der Sar, A. M., Abdallah, A. M., Sparrius, M., Reinders, E., Vandenbroucke-Grauls, C. M., and Bitter, W. (2004). *Mycobacterium marinum* strains can be divided into two distinct types based on genetic diversity and virulence. *Infect Immun.* **72**, 6306–6312.

van der Sar, A. M., Musters, R. J., van Eeden, F. J., Appelmelk, B. J., Vandenbroucke-Grauls, C. M., and Bitter, W. (2003). Zebrafish embryos as a model host for the real time analysis of *Salmonella typhimurium* infections. *Cell. Microbiol.* **5**, 601–611.

van der Sar, A. M., Spaink, H. P., Zakrzewska, A., Bitter, W., and Meijer, A. H. (2009). Specificity of the zebrafish host transcriptome response to acute and chronic mycobacterial infection and the role of innate and adaptive immune components. *Mol. Immunol.* **46**, 2317–2332.

van der Sar, A. M., Stockhammer, O. W., van der Laan, C., Spaink, H. P., Bitter, W., and Meijer, A. H. (2006). MyD88 innate immune function in a zebrafish embryo infection model. *Infect Immun.* **74**, 2436–2441.

Vergunst, A. C., Meijer, A. H., Renshaw, S. A., and O'Callaghan, D. (2010). *Burkholderia cenocepacia* creates an intramacrophage replication niche in zebrafish embryos, followed by bacterial dissemination and establishment of systemic infection. *Infect Immun.* **78**, 1495–1508.

Volkman, H. E., Clay, H., Beery, D., Chang, J. C., Sherman, D. R., and Ramakrishnan, L. (2004). Tuberculous granuloma formation is enhanced by a mycobacterium virulence determinant. *PLoS Biol.* **2**, e367.

Volkman, H. E., Pozos, T. C., Zheng, J., Davis, J. M., Rawls, J. F., and Ramakrishnan, L. (2010). Tuberculous granuloma induction via interaction of a bacterial secreted protein with host epithelium. *Science* **327**, 466–469.

Wang, Z., Gerstein, M., and Snyder, M. (2009). RNA-Seq: a revolutionary tool for transcriptomics. *Nat. Rev. Genet.* **10**, 57–63.

Ward, A. C., McPhee, D. O., Condron, M. M., Varma, S., Cody, S. H., Onnebo, S. M., Paw, B. H., Zon, L. I., and Lieschke, G. J. (2003). The zebrafish spi1 promoter drives myeloid-specific expression in stable transgenic fish. *Blood* **102**, 3238–3240.

Westerfield, M. (2000). *The Zebrafish Book: A Guide for the Laboratory Use of Zebrafish (Danio rerio), 4th ed. University of Oregon Press, Eugene, OR.*

Wienholds, E., Schulte-Merker, S., Walderich, B., and Plasterk, R. H. (2002). Target-selected inactivation of the zebrafish rag1 gene. *Science* **297**, 99–102.

Wiles, T. J., Bower, J. M., Redd, M. J., and Mulvey, M. A. (2009). Use of zebrafish to probe the divergent virulence potentials and toxin requirements of extraintestinal pathogenic *Escherichia coli*. *PLoS Pathog.* **5**, e1000697.

Willett, C. E., Cortes, A., Zuasti, A., and Zapata, A. G. (1999). Early hematopoiesis and developing lymphoid organs in the zebrafish. *Dev. Dyn.* **214**, 323–336.

Wu, Z., Zhang, W., Lu, Y., and Lu, C. (2010). Transcriptome profiling of zebrafish infected with *Streptococcus suis*. *Microb. Pathog.* **48**, 178–187.

Yoder, J. A., Turner, P. M., Wright, P. D., Wittamer, V., Bertrand, J. Y., Traver, D., and Litman, G. W. (2009). Developmental and tissue-specific expression of NITRs. *Immunogenetics* **62**, 117–122.

Zakrzewska, A., Cui, C., Stockhammer, O. W., Benard, E. L., Spaink, H. P., and Meijer, A. H. (2010). Macrophage-specific gene functions in Spi1-directed innate immunity. *Blood* **116**, e1–e11.